EXPERIMENTAL INVESTIGATION OF FISCHER-TROPSCH SYNTHESIS WITH A MODIFIED CATALYST SUPPORT

by

PAWARAT BOOTPAKDEETAM

Presented to the Faculty of the Graduate School of

The University of Texas at Arlington in Partial Fulfillment

of the Requirements

for the Degree of

DOCTOR OF PHILOSOPHY

THE UNIVERSITY OF TEXAS AT ARLINGTON

May 2018

Acknowledgements

I would first like to express my gratitude to my supervising professor Dr. Brian H. Dennis for his support during my Ph.D. study. I am deeply appreciative of his effective guidance, valuable assistance, and continuous support through my study. I would also like to address my gratitude to Dr. Frederick MacDonnell for his precious advice and guidance in chemistry field, and Dr. Kent Lawrence, Dr. Ratan Kumar, and Dr. Zhen Xue Han for serving on my committee.

Moreover, I would like to thank my colleagues from CFD lab and CREST lab, Dr. Wilaiwan Chanmanee, Dr. Olivia Choi, Dr. Jame Grisham, Sandeep Patil, and Mohammad Islam for their friendship, assistance, and support. I would also like to thank my dissertation editor, Joshua Atherton, who helped me reverse my English into something comprehensible.

Lastly, I would like to thank my family for their love and support. Without them, I could not have made it so far in my life.

May 14, 2018

Abstract

EXPERIMENTAL INVESTIGATION OF FISCHER-TROPSCH SYNTHESIS WITH A MODIFIED CATALYST SUPPORT

Pawarat Bootpakdeetam, PhD

The University of Texas at Arlington, 2018

Supervising Professor: Brian H. Dennis

Energy demand has been rapidly increasing in the last 30 years due to the population growth and high demand by industries. However, as natural energy sources are limited, they cannot meet this increased energy demand. Therefore, alternative energies have become an option to sustain current and future energy demands. One promising and reliable alternative energy is the Fischer-Tropsch synthesis (FTS), which is a gas-to-liquid (GTL) technology that converts syngas from a low-value feedstock, for example, from coal, biomass, or natural gas, into a high-value liquid hydrocarbon. In addition, FTS is a highly exothermic catalytic reaction that requires careful thermal management during the synthesis, especially in the catalyst bed, so as to not deactivate the catalyst. One way to manage the increased temperature during synthesis is to use different type FTS reactors. However, these types of reactors do not completely manage the thermal problem of FTS because traditional catalyst materials used during synthesis, such as alumina oxide (Al_2O_3) and silica oxide (SiO_2), do not conduct heat well unless they are specifically modified to do so.

The purpose of this experiment is to increase the thermal capacity of the catalyst support in effort to increase liquid hydrocarbon selectivity. To increase heat transfer,

copper, aluminum, and two sizes of graphite (0.7 and 0.9 mm), were added to the center of 3 mm traditional SiO_2 catalyst support and tested individually. These modified SiO_2 catalyst supports were used in a fixed bed FTS reactor to test for improvements in catalytic performance and product selectivity of the system. The results from these tests were compared with the results from using the traditional SiO_2 catalyst support.

Both the modified and traditional SiO_2 catalyst support were loaded with design catalyst and promoters. The FTS experiment was done at 300 psig, a gas flow rate with 2:1 H_2 to CO ratio, and a catalyst was diluted with quartz chips diluent. The catalytic performance of the four modified and traditional SiO_2 catalyst support was determined after the synthesis reaction stabilized around 18-20 h. after the activation started. The products, gas outlet, oil, and a water-alcohol mixture, were used to estimate the catalytic performance of the catalysts.

The results show the increased of a catalytic performance of the modified SiO_2 catalyst support with a Cu core affected by the increase in an overall heat capacity in a catalyst pellet. The improvement of the overall heat capacity showed only a small temperature swing in the system which resulted in about 30% increased in overall catalyst productivity. A spent modified SiO_2 supported catalyst with a Cu will be characterized using TEM and XRD to see the synthesis reaction affect the catalyst particles

Table of Contents

List of Illustrations

List of Tables

Chapter 1

Introduction and Literature Review

Nowadays, energy is the most important factor driving the world forward. Massive amounts of energy are used in all industries to support the needs of people. In fact, little can be accomplished in daily life without access to plentiful energy. Accordingly, energy demand has rapidly increased in the past 30 years due to large increases in population and industries. The International Energy Outlook 2017 (IEO2017) predicted that the world energy consumption would increase by 28% in the next 20 years. The IEO2017 predicts that the world energy consumption of all fuel sources will increase except for coal and liquid fuel energy, which they believe will remain constant. In addition, petroleum-based liquid fuels, the largest current and future energy source according to the IEO2017, but its relative share as a source of energy may slightly decrease as people search for alternative energies. Indeed, the use of non-fossil fuel type energies, such as renewables and nuclear, will increase around 2.3% per year, the largest increase of use of any other type of energy source. However, according to the IEO2017, fossil fuels will still account for nearly three-quarters of the world's energy consumption through 2040. The global consumption of natural gas is expected to increase to about 1.4% per year compared to other fossil fuel energy because of its low carbon intensity, relative abundance, and ease of production [1]. Nevertheless, the increase of world energy demand and the limitation of energy supplies will lead to an increase in the price of energy, creating a need to develop more alternative energies. This has led to the development of synthetic fuels.

Fischer-Tropsch Synthesis (FTS) is a promising and reliable alternative energy that uses a technology called gas-to-liquid (GTL) to convert synthesis gas (H_2 and CO) into a long-chain hydrocarbon. The schematic diagram of FTS can be seen in Figure 1-1.

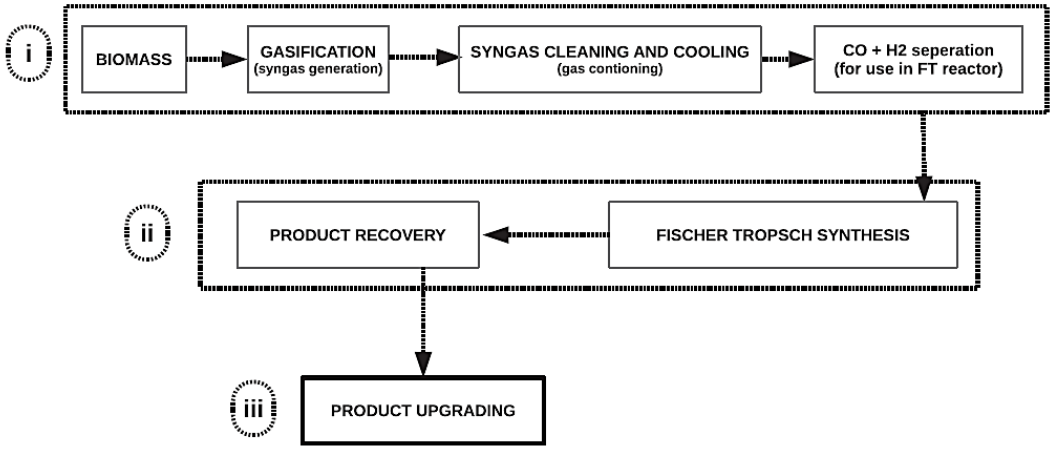

Figure 1-1 Overall flow schematic for FT synthesis: i) syngas generation via biomass gasification, ii) syngas conversion to higher hydrocarbons via FT reaction, and iii) separation and refining of FT yield to useful products [2].

A large-scale size FTS plants usually facilitate with CH_4 reforming, coal gasification, and biomass as a syngas generator to the system. Therefore, the need of FTS is increasing as a result of increases in energy demand and also the environmental concern by reducing the pollution generated by the fossil fuel. Since the FT fuel exhibits lower emission, nitrogen, and sulfur than gasoline and diesel when it uses in the engine or machine [2].

1.1 History of Fischer-Tropsch Synthesis

The Fischer-Tropsch synthesis (FTS) was developed in 1925 by Franz Fischer and Hans Tropsch at the Kaiser-Wilhelm-Institut für Kohlenforschung in Mülheim an der Ruhr, which is now the Max Planck Institute for Coal Research in the present day. The synthesis was intended to generate hydrocarbon molecules and turn them into fuel by using coal-derived gas as a feedstock. During FTS, the gas feedstock from a coal-derived gas with hydrogen (H_2) and carbon monoxide (CO) composition is converted into the liquid product (middle distillates) and wax at atmospheric pressure. In the beginning, the mixed gas from

the coal-derived gas feedstock was first processed using an iron (Fe) catalyst. However, because they provided a higher hydrocarbon product, cobalt (Co) and Nickel (Ni) were more commonly used as catalysts in FTS. In addition, the cobalt medium pressure synthesis was later developed by Fischer and Pichler. The major product from this synthesis is middle distillate and wax. After that, many countries became interested and began focusing on FTS research and development [3]. In 1933, the first pilot plant was built in Oberhausen, Germany under the Ruhrchemie AG. Here, the FTS operation was conducted at atmospheric pressure using a fixed bed reactor and Co as the catalyst. Because of high demand for oil during World War II, industries and governments heavily supported FTS research and development. In fact, FTS synthesis became a significant energy source in Germany due to the petroleum reservoir shortage problem. However, during this time much research showed that the Ni catalyst was not practical to operate on a big scale and it gave a high methane (CH_4) yield during synthesis. Then in 1937, Fe was used to replace the Co catalyst by Fischer and Pichler because of the increased cost of Co and the increase of the Fe catalytic performance when operate in pressure between 5-20 atm. In the 1950s, SASOL FTS company was successful running an FT plant by using a Fe catalyst in fixed-bed with recycle unite successful in South Africa up until present with a high yield of an α-olefins. The research in the FTS was continue with the interest in improving productivity of selectivity of the FT system by testing different catalyst, developing the catalyst support, and improving the system efficiency and reactor.

1.2 FTS Catalyst

In FTS, most of the metals from group VIII (transition metal) in the periodic table, Co, Fe, Ni, and ruthenium (Ru), show the most activity in hydrogenation between H_2 and CO in gas-to-liquid (GTL) industries. Ni is the most reactive catalyst in the CO

hydrogenation process; however, CH_4 is the majority product of this catalyst, especially at a high temperature [4]. At a low temperature, nickel carbonyl volatile can be formed and cause the catalyst to be damaged during the synthesis. Therefore, only Co, Ru, and Fe remain as a choice. However, getting the right catalyst for synthesis needs to take into account many perspectives, for example, cost, availability, the desired product, catalyst lifetime, and activity. Ru is a suitable catalyst for the olefin synthesis; however, in the great quantities that industries require, synthesis could be a problem because the cost per unit of Ru is quite expensive (about 31,000 times when compared with Fe) and the availability is quite low. Thus, the choice is narrowed down to Fe and Co, which are currently the most used in FTS.

1.2.1 Iron Catalyst

Fe is the most common catalyst choice in the FTS industry because of the high availability and lower price (about 230 times) when compared with Co. The active phase of the Fe catalyst is obtained after Fe oxide is reduced under the H_2. Most of the oxide particles turn into a different phase of iron carbide after reduction. The Fe catalyst requires low temperature during the synthesis because the phase changing happens to the Fe particle (the carbide formation) at high temperature. The activity of the Fe catalyst is gradually decreased over time on steam, and many factors can cause the early deactivation of the catalyst, for example, from heavy carbon residue, sintering, area loss, oxidation, coking, and catalyst poisoning from the sulfur component of H_2S. In fact, the Fe catalyst is easy to get deactivated from sulfur poisoning as compared with the Co catalyst. Poisoning is a problem in the FTS because a small amount of sulfur can cause a rapid deactivation of the FT catalyst. Hence, it is a trade-off between deactivation and the cost of the catalyst. Another bad side effect of using Fe as a catalyst during the synthesis is the

water gas shift reaction (WGS) is the main reaction. The WGS reaction provides more H_2 to the system, which is only good when using coal-derived gas as a feedstock.

1.2.2 Cobalt Catalyst

Co is another commonly used catalyst in the FTS industry due to high resistance to deactivation, even though it has a higher price when compared to the Fe catalyst. At first, the Co catalyst was prepared by coprecipitating the cobalt nitrate and thorium (Th), zirconium (Zr), or magnesium (Mg), with the solution onto kieselguhr to make a mixture of oxide support on kieselguhr. Since Co has a higher cost than the Fe catalyst, during the catalyst preparation, the appropriate treatment was used to reduce the amount of Co content on the support and increase the high Co metal surface at the same time [5]. Therefore, the Co catalyst required a more narrow operation range of a low-temperature Fischer-Tropsch (LTFT) and pressure than the Fe catalyst. At the slight change in these conditions, the product distribution in the system can be changed into light or heavy hydrocarbon, like CH_4 and wax. However, the Co catalyst still benefits the system because it has less effect on the WGS reaction, meaning it can be ignored during the synthesis.

1.3 Product Distribution

Product distribution in FTS can be described as the polymerization of the hydrocarbon chain. The ratio of usage between H_2 and CO is the indicator of product distribution from the synthesis. Hence, the stoichiometric reaction can be obtained when the ratio of H_2 and CO are between 1.8 to 2.1. Many reactions take place in the FT synthesis, but the exact reaction can never really be identified. However, the simplified equation can be shown as [6]:

Paraffins: $(2n+1)H_2 + nCO \rightarrow C_nH_{2n+2} + nH_2O$

Olefins: $2nH_2 + nCO \rightarrow C_nH_{2n} + nH_2O$

Alcohols: $nCO + 2nH_2 \rightarrow C_nH_{2n+2}O + (n-1)H_2O$

where the reaction can develop into a wide range of different carbon number (n) products. The side reaction can be shown as:

Methane: $CO + 3H_2 \rightarrow CH_4 + H_2O$

Water gas shift (WGS): $CO + H_2O \leftrightarrow CO_2 + H_2$

Therefore, paraffin are the primary products for the FTS. The chain growth of the paraffin can be simply explained by using the Anderson-Schulz-Flory (ASF) equation:

$$\log(W_n/n) = n \log\alpha + \text{constant}$$

where W_n is the mass fraction of the species with carbon number n. From the slope of the plot of $\log(W_n/n)$ against n, the value of α is obtained.

As shown in Figure 1-2, the plot normally yields a straight line with a carbon number between C_3 to C_{12}, which confirms that the chain growth probability is a constant in this range. The ASF plot bends around C_{10} to C_{12}, creating another straight line from the high alpha value (α_2) because the waxes that are produced cause the catalyst pores to fill up with emulsion from vapor/liquid hydrocarbon. Chain growth probability shows that the longer the gas resides inside the catalyst particle, the longer the chain of the product grows due to the readsorption of the alkenes and continued chain growth. If the chain is long, the ratio between alkene/alkane is low because of the secondary hydrogenation during the readsroption process [5].

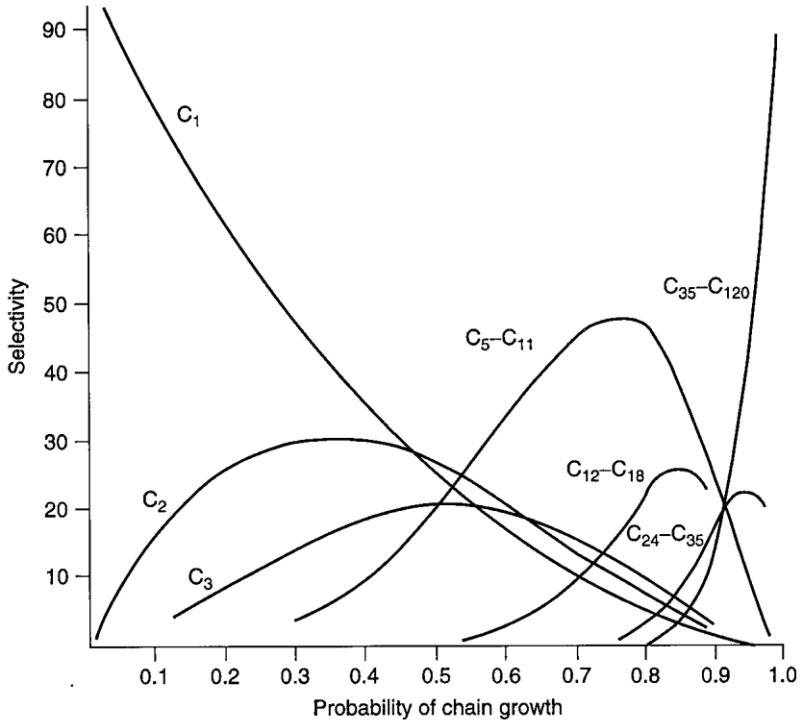

Figure 1-2 The relation between selectivity of FT hydrocarbon products as a function of the probability of chain growth (α), assuming α to be independent of chain length [5].

1.4 Fischer-Tropsch Chemical Reaction and Reactor

1.4.1 Fischer-Tropsch Synthesis Chemical Reaction

The chemical reaction generated during the FTS is a broad distribution of products according to the carbon number. The potential reactions are highly exothermic as shown below:

$$2n\ H_2 + n\ CO \rightarrow -(CH_2)_{-n} + n\ H_2O \qquad \Delta_R H°_{250°C} = -158.5\ kJ/mol\ (n=1)$$

This main reaction will lead to alkanes (paraffins), alkenes (olefins), and alcohols formation during the synthesis as shown below:

$$(2n+1)H_2 + nCO \rightarrow C_nH_{2n+2} + nH_2O$$

$$2nH_2 + nCO \rightarrow C_nH_{2n} + nH_2O$$

$$nCO + 2nH_2 \rightarrow C_nH_{2n+2}O + (n-1)H_2O$$

Water gas shift is the significant product for FTS especially with an Fe based catalyst and K promoter. However, this reaction can be ignored when Co or Ru is used as the catalyst.

$$CO + H_2O \leftrightharpoons CO_2 + H_2 \qquad \Delta_R H°_{250°C} = -39.5 \text{ kJ/mol}$$

Methanation and Boudouard reactions are undesired reactions that cannot be ignored:

$$3\,H_2 + CO \rightarrow CH_4 + H_2O \qquad \Delta_R H°_{250°C} = -213.0 \text{ kJ/mol}$$

$$2CO \leftrightharpoons CO_2 + C \qquad \Delta_R H°_{250°C} = -175.6 \text{ kJ/mol}$$

The equation above shows that the system generates a large amount of reaction heat, which makes the FT a highly exothermic experiment. Sie and Krishna showed that the exothermic reaction from methanation could raise the adiabatic temperature of the system to about 1600K if the system did not properly control the temperature [7].

1.4.2 Fischer-Tropsch Synthesis Reactor

The FTS reactor went under rapid development by Germany until the first commercial plant was established around 10 years before the WWII [8]. Many reactor types were developed to be able to handle heat generated from the FTS reactions. Recirculate the residue gas was one of method used to manage heat in the system and it also enhances heat transfer in a catalyst bed as well. Only 3 types of reactor (tubular fixed bed reactor, slurry phase reactor, and fluidized bed reactor) are used in the commercial unit nowadays.

In the FTS, an average heat release from n CH_2 formation is around 145 kJ, the sufficient heat removal from the catalyst bed is required to maintain adiabatic operation in the system [9]. The heat transfer from catalyst particles to the heat exchanger can be removed by using cooling water, and the steam generated from the heat removing process can be used to generate steam. The FTS reactor can be divided into two modes: a low-temperature FT (LTFT) mode that operates at 200-240°C and a high-temperature FT (HTFT) mode that

operates at 300-350°C. At the high temperature, the chain length probability (α) of the product will be lower. Then LTFT is suitable for a product with long-chain hydrocarbons such as liquid fuel and wax, while HTFT is more suitable for lower olefins and gasoline [10]. The first FTS reactor was vertical metal sheets with horizontal cooling tubes crossing the sheets. The catalysts is loaded between sheets and tubes which was difficult and took long time to load [11]. The heat generated is removed by the plates and cooling tubes. This type of reactor was difficult to manufactore to handle the operation at high pressure. Moreover, the idea of hydrocarbon products are produced at atmospheric pressure while oxygenated products are produced at higher pressure, made the first generation FTS reactore operated at low pressre or 1 atm [3] [7].

During the time the first FTS reactor was being developed, researchers also created a multiple tubular fixed bed reactor that operated with higher pressure (between 10-15 bars). This reactor has better heat removal from the catalyst bed than the first type of FTS reactor, but it had a high manufacturing cost and loading the catalyst into the system was more difficult.

There are three types of FTS reactors used on a commercial scale: the tubular fixed bed reactor, slurry phase reactor, and fluidized-bed reactor (Figure 1-3).

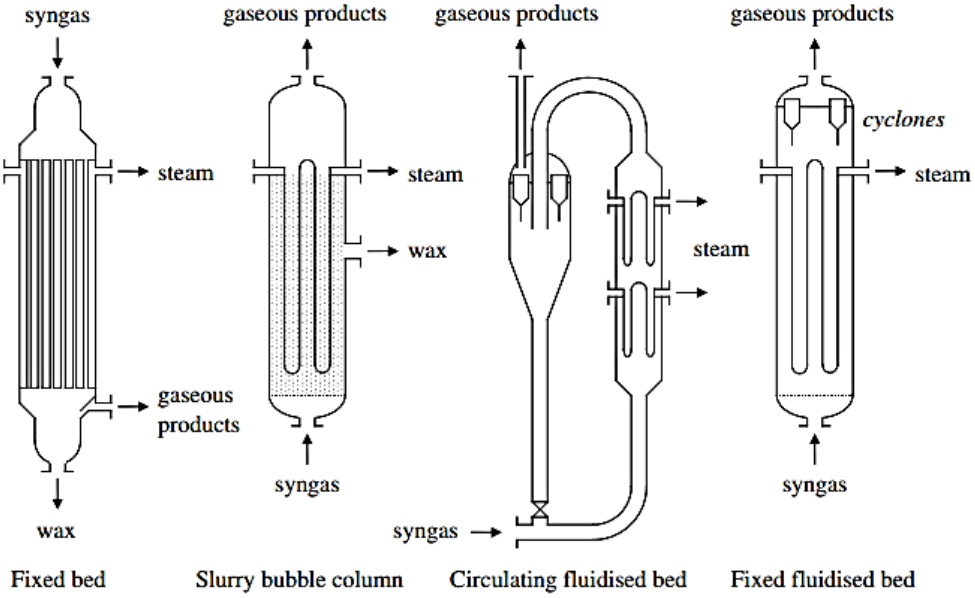

Figure 1-3 Type of commercial use Fischer-Tropsch reactors at present

1.4.2.1 Tubular fixed bed reactor

Process industries have been using the fixed bed reactor for quite a long time. At first, the fixed bed reactor was only found in commercial use because the limitations of technology at that time meant it was the best type of reactor. However, now the fixed bed reactor is also used in research and for other purposes. This reactor contains the pellet form of catalyst packed in its static bed. The gas passes through the catalyst bed and reacts once the catalyst and gas are in contact. The reaction inside the reactor is limited by the surface area of the gas passing through. The limitations of this reaction can be solved by increasing the number of the reactor tubes. The catalyst pellet does not require much strength since the catalyst bed is not moving. However, the heat generated from exothermic reactions requires sufficient heat removal. To help remove heat faster, the distance between the

catalyst pellets and the tube wall can be shortened so the reaction heat can be removed from the outside of the reactor tube wall [5]. In a tubular fixed bed reactor has smaller heat conductivity and heat transfer from catalyst pellet to the tube wall when compare with fluidized bed reactor, which will give unstable temperature inside the catalyst bed. The causing of the temperature raising can harm the catalyst that leads to decreasing of selectivity, syngas conversion, and inactivity in a FTS catalyst [7]. Recirculation of tail gas is a standard procedure in order obtain high overall syngas conversion.

1.4.2.2 Slurry phase reactor

Various sizes of slurry phase reactors with low gas space velocity were tested during the 1950's and 1960's in Germany, England, and the USA. The slurry phase reactor with low operating temperature is suitable for wax production because the liquid wax works as the medium to suspend the catalyst particles. However, the essentials of product separation between wax and catalyst particle were not developed until later. The slurry phase reactor gives very high activity and conversion rate at smaller catalyst loading because it has a smaller particle size that causes high activity per unit mass. Nevertheless, the slurry phase reactor conversion is not as good as a fixed bed reactor since the smaller particle size does not have any advantage over the lower loading [5] [12].

1.4.2.3 Fluidized-bed reactor (bubbling or circulating fluidize bed)

The fluidized-bed reactor contains catalyst particles in a fluid state [12]. Their catalyst was suspended in the inert liquid mineral oil so that the catalyst particles could be in contact with the reactant gas feed through the reactor. Because the gas can thoroughly contact the catalyst particles and provide increased surface contact area, using a fluidized bed reactor helped to solve the mass-transfer limitation problem that happens in fixed bed reactors [12]. Moreover, the fluidized bed also help with the heat transfer problem by reducing the heat gradient build-up by the stationary bed. The fluidized bed can operate

almost isothermally with the internal tubes through which circulated heat transfer fluid can help to remove the excess heat. The catalyst in a fluidized bed reactor can be replaced without shutting down the reactor, unlike the fixed bed reactor that needs to be shut down every time the catalyst regenerates or needs to be added [7].

Chapter 2

Traditional Catalyst Support and Preparation

2.1 Introduction

The FTS is a highly exothermic polymerization process of the hydrocarbon product for the gas to liquid (GTL) industry. Catalytic material and support, the synthesis procedure, choice of the reactor, and the process condition (e.g., syngas composition, the residence time of the feed in the reactor, reactor pressure and temperature) are the factors involved in the FTS process. The FTS factors control the syngas conversion, hydrocarbon selectivity, and the product distribution of the synthesis [13]. Hence, each factor in FTS should be carefully selected to have optimum condition during the synthesis. Therefore, the reactor, process condition, and the synthesis procedure are not easily modified after the design and fabrication process. However, the catalyst material and support are highly modifiable and have many possible factors that can be developed. The catalyst metal is chosen according to the design product, and it usually comes from group VIII in the periodic table (Co, Fe, and Ru), as discussed in chapter 1. However, the catalyst metal is not the only key factor in the FTS. Other important factors to consider are the catalyst promoter, support material, preparation method, and catalyst pretreat method.

2.1.1 Catalyst Promoter

Catalyst promoter is the second metallic material that can be deposited together with or after the main catalyst metal. The sequence of the impregnation depends on the design process during the incipient wet impregnation method. The main purpose of the catalyst promoter is to help enhance the distribution and dispersion, and reduce the agglomeration of the catalytic material before and after the synthesis.

In general, the active phase of the catalytic material used in the FTS is the metallic form of Fe or Co, which oxidize when they contact the air. Hence, the catalyst requires a reduction

step under H_2 atmosphere to change the oxide phase of Fe or Co to a metallic phase prior to the synthesis. In the reduction step, heat is applied to the reactor under the H_2 atmosphere to change the oxide form; in this case, Co oxide (CoO, Co_2O_3, and Co_3O_4) is turned into Co metal (Co^0). The promoter, for example, Ru, Platinum (Pt), or Rhenium (Re), is introduced to the Co catalyst to help in the reduction process by reducing reduction temperature. The promoter is added to help Co produce more Co^0 surface sites by facilitating the reduction of cobalt species that interact with the catalyst support [14]. Different types of promoters change the functions in the Co catalyst, for example, enhance activity, reduce cobalt crystal size, and reduce methane selectivity. Thus, the function that will happen in FTS depends on the promoter used in the system.

2.1.2 Catalyst Support

The catalyst support material plays an important role in the FTS by increasing and extending the catalytic activity. The catalyst support material should be stabilized under process condition (operation, start-up, and shutdown). The degradation of catalyst support during the process could cause partial or total blockage inside the reactor tubes that might cause hot spots, hot bands, or totally hot tubes. Moreover, in order to optimize synthesis, the physical properties and structure of the catalyst support should:

- Have high acidity to disperse and stabilize the active catalyst phase, which affords a high activity and stability.

- Be porous to increase both activity and hydrocarbon selectivity in the active phase of the catalyst, which can increase the output of oil. In addition, the pore size should be medium to limit product distribution to the optimal range.

- Consist of highly thermal conductive material to dissipate reaction heat, especially when the catalyst is operated in a fixed bed reactor, to avoid overheating the system.

- Have high mechanical strength during the operation of a slurry bed reactor so it will not break down.

- Have small particle size so that it can modify the electronic properties of the active phase due to the electron deficiency, which changes the absorption behaviors of CO and H_2 [15].

Different types of catalyst support interact with different catalysts in various ways and have a range of metal-support interaction that affects the reducibility of the catalyst under the H_2 atmosphere. At a high metal-support interaction, it is difficult for Co to reduce from cobalt oxide (Co_3O_4 and CoO) to cobalt metal (Co°) and could lead to inactivity in the Co-silicate or aluminate formation because they have high thermal stability but low CO dissociation. However, a high metal-support interaction promotes catalyst dispersion over the surface because the catalyst prefers to attach to the support surface rather than particles with the same species. At a low metal-support interaction, sintering of the catalyst metal causes the deactivation of the catalyst. One cause of the sintering is the agglomeration of Co metal over the support surface from the low metal-surface interaction. Another cause of the sintering is the over-heating of the catalyst bed during the synthesis. In order to avoid the common problems associated with high and low metal-support interaction, most researchers use a catalyst support that has medium metal-support interaction. The following table shows the strengths and weaknesses of the different catalyst supports:

Support type	Advantage	Disadvantage
Aluminum oxide (Al_2O_3)	- Strong mechanical strength - High surface area - High Co dispersion on surface	- High metal-support interaction - Small Co particle size (Co particle size decrease after deposite) - Low reducibility
Silica oxide (SiO_2)	- Weak metal-support interaction - High reducibility - Large Co particle size - High surface area	- Low Co surface dispersion
Titanium oxide (TiO_2)	- Better mechanical strength and properties - Large Co particle size	- Strong metal-support interaction - Low reducibility - Low surface area

2.2 Material, Method, and Characterization

In the FTS, multiple methods are used to determine efficiency and productivity of the system, for example, surface area analysis, surface morphology, catalyst particle size, gas composition, and liquid oil composition. Hence, different types of equipment must be used in the analysis of the catalyst and product from the synthesis. Physical characterization is done to the catalyst prior to and after the synthesis to compare how the synthesis affects the catalyst, support, and products during the synthesis.

2.2.1 *Brunauer-Emmett-Teller (BET) Surface Area and Porosity Measurements* [16]

Brunauer-Emmett-Teller, commonly known as BET, surface area analysis is used to determine the surface area, pore volume, and pore size of the support. BET surface area analysis determines internal and external surface area based on the physical gas

absorption according to the Brunauer-Emmett-Teller method [17] [18]. The volume of nitrogen gas adsorbed on the particle surface is measured at the nitrogen boiling point (-196°C). At this temperature, nitrogen gas is being condensed on the particle surface because the temperature is below the critical temperature of the gas (-146.9°C). After this, the correlated amount of the surface area can be determined because the gas-particle size and the absorbed gas are known, and surface area and the volume of the particle can be calculated from the interpretation of the data. This analysis starts when the gas (adsorptive) is pumped into a sample tube. The gas will cover the outside layer of the particle and go through the accessible surface. Then, the amount of gas used to cover the monolayer surface can be calculated from the isotherm absorption by using the following BET equation [19] [20]:

$$\frac{p}{n_a(p_o - p)} s_{total} = \frac{1}{n_m C} + \frac{(C-1)}{n_m C} \cdot \frac{p}{p_o}$$

where

n_m is the monolayer capacity

C is the BET constant

p is the equilibrium and p_o is the saturation pressure of adsorbates at the temperature of adsorption.

n_a is the adsorbed gas quantity (in volume units)

Mesoporous (pore size between 20-500Å) catalyst support is the most common catalyst size for the FTS since the product will change according to the support pore size. The synthesis favors the CH_4 product when the pore size is too small (microporous, pore size < 20Å). On the other hand, the synthesis will favor long chain hydrocarbon formation when the size of the pore is too big (macroporous, pore size > 500Å). Hence, the mesoporous

catalyst support helps to obtain the liquid hydrocarbon with the carbon number between c_5 to C_{18} [21].

2.2.2 Thermogravimetric Analysis (TGA)

Thermogravimetric analysis (TGA) is used to measure the weight/mass change (loss or gain) of a sample as a function of temperature, time, and atmosphere. The measurement is used to determine phase transition and thermal stability. TGA is used to characterize decomposition, oxidation, and reduction from the weight change of a sample. The TGA method can help determine the following information from a sample:

- thermal stability
- oxidative stability
- composition
- estimated lifetime
- decomposition kinetics
- the effect of reactive or corrosive atmospheres
- moisture and volatile content

As mentioned above, the weight change during TGA could either be a loss or a gain. The weight gain of a sample during TGA occurs due to oxidation, in which the sample interacts with an oxidized atmosphere, and absorption. The weight loss of a sample during TGA occurs due to decomposition, evaporation, reduction, which is the interaction between the sample and a reducing atmosphere such as H_2 and ammonia, and desorption. The rate of reaction in TGA comes from the kinetic process of a sample. Hence, a TGA analyzer must be accurately calibrated and operated by controlling the heating rate of the furnace, measuring the change in temperature (obtained from the thermocouple), and measuring the weight/mass change while the sample is heating up or held at isothermal temperature [22].

2.2.3 Temperature Programmed reduction (TPR)

Temperature Programmed Reduction (TPR) is a technique used to evaluate the reduction state of a heterogeneous catalyst under H_2 atmosphere. TPR provides details about the degree of phase-support interaction and the extended reduction of different catalysts and phases at different temperatures. The typical TPR apparatus is assembled with 3 parts i) a gas line for pretreatment and analysis; ii) an electronically controlled reactor; and iii) a quantitative evaluation detector of a gas-consumption. The analysis is operated at ambient (in flowing gas) or sub-ambient (under vacuum) pressure. The detector (TCD; Thermal Conductivity Detector) graphs changes during the analysis, for example, the pressure change of the reaction gas and the weight change of the sample, depending on the settings of the TPR being used. The output signal from TPR is proportional to the input gas concentration (the mixture of H_2 in the carrier gas) [23]. Hence, the reducibility obtained from TPR is determined by O_2-titration ($\%R_o$) as shown below

$$\%R_o = \frac{no.of\ mole\ O_2\ uptake}{stochiometric\ no.of\ O_2\ mole}\ x\ \frac{3}{2}\ x\ 100$$

From the equation, the Co particle is assumed to have complete re-oxidation from Co to Co_3O_4 ($3Co + 2O_2 \rightarrow Co_3O_4$). The value obtained from TPR in the form of a graph is used to determine the reducibility (R_H) of the catalyst by using the following equation

$$\%R_H = \frac{area\ of\ \beta\ peak}{sum\ of\ area\ of\ \alpha, \beta, \gamma\ peaks}$$

where α, β, and γ are the reduction peaks assigned to nitrate, Co_3O_4, and cobalt-aluminate or silicate respectively in the TPR profile of the supported catalyst [24].

2.2.4 Scanning Electron Microscopy (SEM)

Scanning Electron Microscope (SEM) is a technique used to analyze the surface structure and morphology of a sample in the micro- to nano- meter scale. SEM is a type of microscope that produces images from electrons bounced off the surface of a sample. The

gun beam scans over the sample surface and shoots electrons onto the surface. The electrons from the gun interact with the atoms on the surface sample. This interaction between the electrons and surface atoms is converted into a signal that includes the morphology (texture), chemical composition, and crystal structure and orientation of the structure of the material. Data from SEM are collected over a small area, approximately 5 microns to 1 cm, with a magnification range from 20X to around 30,000X, which gives a resolution around 50 to 100 nm. Moreover, the chemical composition can be qualitatively determined by using EDS (Energy-Dispersive X-Ray Spectroscopy) and EBSD (Electron Backscatter Diffraction) for the crystal structure and orientation. EDS detects energy emitted from the sample after the interaction with the electron beam. The sample emits a wide range of energy, such as x-rays, which is detected and analyzed by the system software to determine particular elements within their range of energy. EDS is used to determine the chemical composition of sample material from a few microns to a cm spot size area. The composition can be mapped over a large area that details the sample composition by element, for example, silicon element on silica oxide support [25].The crystalline material analyzed under SEM can diffract the accelerated electrons from the primary electron beam. Changing the crystalline structure and the crystallographic orientation of the sample changes the diffraction pattern, which can be used to see the geometry of the lattice plane in the crystal from where they originate [26].

2.2.5 Transmission Electron Microscopy (TEM)

Transmission Electron Microscopy (TEM) is a type of microscope technique that provides morphologic, compositional, and crystallographic information similar to the light microscope, except TEM utilizes energetic electrons. TEM provides two-dimensional high-resolution images that can go as low as 1 nm. The images are produced from the interaction between the sample and energetic electrons in a vacuum chamber. The vacuum

chamber gives the ability and space for the electrons to move while interacting with the sample. After the electrons interact with the sample, they move through electromagnetic lenses and solenoids, and contact with a screen where they are converted into images. Adjusting the voltage of the electron gun controls the speed of the electrons, which is used to provide sharper images. The voltage of the electron gun changes the speed of the electrons, which changes the electromagnetic wavelength at the solenoids. Since the speed of the electrons and the electromagnetic wavelength are correlated, the shorter wavelength gives the greater image quality and detail. The different dark/brightness of the image shows the ability of the electrons to pass through the sample, and these differences provide details about the structure, texture, shape, and size of the sample. The TEM technique provides more detail than other optical microscopes; however, TEM is limited by the thickness of the sample. The sample thickness should be thin enough for electrons to pass through, which is known as electron transparency. Moreover, the sample needs to be able to withstand the high vacuum inside the chamber and dehydration, cryofixation, sectioning, staining, and sputter coating for non-conductive materials.

2.3 Preparation Method

Preparing active catalyst products from catalytic materials is a sophisticated process that takes many steps. The heterogeneous catalyst is the majority catalyst used to convert gas into liquid products where a surface reaction between reactant gases and a solid catalyst (heterogeneous catalyst) takes place. The heterogeneous catalyst can be distinguished into three types i) bulk catalyst and support, ii) impregnated catalyst from preformed support, and iii) mixed agglomerated catalyst.

i) Bulk catalysts are mainly composed of active substances. The preparation of bulk catalysts is a similar procedure as preparing alumina, silica, and alumina-silica support. In

some cases, an inert binder is added to the bulk catalyst to aid the forming and shaping operation.

ii) Impregnated catalysts from preformed support are impregnated blank catalyst supports with an active metal phase; for example, impregnated cobalt nitrate on silica oxide support.

iii) Mixed-agglomerated catalysts are obtained by agglomeration of the mixture between an active metal phase and a powder support or support precursor.

However, impregnated catalysts from preformed support are the most widely used in FTS because they lead to bifunctional catalysts, a high dispersion of the active phase, better diffusion of gases through the catalyst bed, better mechanical resistance to a moving or fluidized bed reactor, better thermal conductivity, improved catalyst properties induced by active phase-support interaction [27]. In addition, heterogeneous catalysts could be affected by several parameters during the preparation process, such as the amount of solution used during the impregnation and the volume of catalyst support [28]. Many complicated preparation sequences can be used during the catalyst preparation process, and every sequence needs to be carefully performed with proper protocol in order to eliminate any problems the catalyst product might encounter. Several preparation processes could be applied depending on material choices during the process and the final desired (chemical and physical) characteristic of the products.

The goal of the catalyst preparation process is to produce and reproduce stable, active, and selective catalyst products, and using impregnated catalysts is a common and effective way to do so. To impregnate catalysts, the following steps are followed:

1. Soak the catalyst support in the impregnation solution for the amount of time necessary for the desired absorption.

2. Dry the catalyst support until all of the absorbed impregnation solution has evaporated.

3. Eliminate the catalyst precursor by calcination and activate the catalyst by reduction or another appropriate procedure.

2.3.1 Catalyst Support Impregnation

The first step to impregnate a catalyst is to bind the catalyst particles to the catalyst support by immersing the catalyst support into the impregnation solution. There are two methods to impregnate a catalyst: 1) with excess solution or 2) with repeated application of the solution, also known as the dry impregnation or incipient wet impregnation method.

1) In the excess solution method, the catalyst support is first soaked in a liquid solution until the catalyst support is saturated. After drying the catalyst support, it is resoaked in the liquid solution. This process is repeated until the desired amount of catalyst content is bound to the catalyst support. However, the catalyst support must have a strong enough structure to withstand the repeated soaking for this method to produce desirable results.

2) In the incipient wet impregnation (IWI) method, the catalyst support is soaked in an amount of impregnation solution that is equal to or slightly less than the amount of the catalyst support pore volume. Unlike the excess solution method, in this method, the catalyst support is only soaked once. This method is good in controlling the amount of catalyst precursor that is bound to the catalyst support; however, it has poor distribution of the catalyst over the surface. This method is suited to impregnate catalysts with high metal loading [29].

2.3.2 Drying Method

The drying method is used to completely evaporate the impregnation solution (mostly water) from the catalyst support pores [30]. In order to increase the efficiency of FTS, the catalyst is required to have a high porosity and surface area. The catalyst with high porosity and surface area is prepared by IWI for use in FTS. However, if the impregnation solution remains inside the catalyst, i.e., it is not completely evaporated, the

porosity and surface area of the catalyst support will be damaged; for example, the surface area and pore volume will be reduced and the porous structure will be changed. These damages are the result of:

- the collapsing of the interior structure (loss of surface area and pore volume) from an increase of internal pressure and capillary stress inside the catalyst support; and

- the agglomeration of cobalt particles from a precipitation of solid cobalt particles from the remaining solution in low [31].

These destructive effects can be minimized by increasing the evaporation rate of the impregnated solution during the drying method. The evaporation rate is maximized by lowering the drying temperature, increasing the relative humidity of the drying medium, and/or reducing the air flow through the drying bed [32]. Moreover, the nucleation and growth of cobalt oxide occurs if the catalyst is dried at a high temperature, which increases the possibility of aggregation. Co particles averaging around 9 nm can aggregate into a cluster from 13 to 80 nm in size. The bigger the cluster, the more it affects the selectivity of FTS. The larger clusters exhibit higher selectivity toward long-chain alkenes and higher olefin formation due to readsorption and secondary chain growth. Despite this, Co particles being close together increases the deactivation of the catalyst; for example, some evidence shows that the distance of the interparticle has a significant effect on the stability of copper catalyst for methanol synthesis [33]. Thus, the nanoscale distribution of the catalyst particles is an important design parameter of the supported catalyst and can be optimized by carefully controlling the temperature and drying medium during the drying method. Hence, many drying methods, such as the air-dry, vacuum-dry, nitrogen-dry, and freeze-dry methods, have been introduced during the catalyst preparation to increase selectivity toward the desired synthesis product and protect the catalyst from early deactivation.

2.3.3 Calcination Method

Calcination uses heat to treat the catalyst material in order to eliminate the salt catalyst precursor content in the catalyst compound and stabilize the catalyst particles. The catalyst calcination method is usually used to treat the catalyst in an air atmosphere. This method is similar to the drying method; however, it has to be done at a higher temperature than the operating temperature in order to decompose the salt precursor content that contains cobalt particles, for example, nitrate, chloride, acetate, and ammonium. The calcination temperature depends on the choice of precursor used during the impregnation. Much like in the drying method, the temperature used during the calcination method affects the catalyst dispersion. Calcination causes the catalyst metal particles to sinter at high temperatures when the cobalt particles migrate over the catalyst surface and form one particle from 100 to 200 nm in size. Hence, calcination temperature should be optimized to eliminate all of the salt precursor and maintain the uniform dispersion over the catalyst surface. Moreover, calcination reduces the phase change of the support and catalyst when it is operated at the desired temperature. Finally, to help maintain uniform dispersion of the catalyst over the support during calcination, the temperature ramp must be optimized. Even though the catalyst needs to calcine at a higher temperature than the decomposition of the precursor, a low and slow heating rate helps reduce the migration of the cobalt particles and the thermal shock that happens when the temperature suddenly changes.

2.3.4 Reduction Method

In the reduction method, the activating the catalyst leads to the nanoparticle formation. The reduction method has a significant influence on the final nanoparticle size. The reduction is affected by the interaction between the metal and the surface. This method is done at a high temperature in a hydrogen atmosphere, which leads to the uniform dispersion of the catalyst particles. The catalyst requires temperature high enough to

maintain this uniform dispersion of the particles, but low enough to reduce metal-surface interaction and avoid sintering [34]. In order to determine the proper reduction conditions, many methods can be used, for example, temperature programmed reduction (TPR) and chemisorption. These methods are used to determine the most suitable temperature, degree of reduction of each catalyst, and extent interaction between the surface and the metal oxide during the reduction [35]. In addition, the gas flow and the heating rate of the reduction process can also affect the degree of reduction as well. Munnik et al. [33] explain that the gas flow and heating rate affect the activity of the catalyst during the reduction especially at a high heating rate, which causes the activity of the catalyst to reduce. The gas flow and the heating rate affect the phase formation of the catalyst during the reduction, which is caused by differences in mass transfer at different support and pore sizes. Since transforming the oxide into a metal or carbide form is slower than transforming them back to the oxide, the catalyst requires a lower heating rate and slower gas flow during the reduction in order to uniformly transform the oxide cobalt into the cobalt metal [36].

Chapter 3

Parametric Study in Catalyst Preparation

This chapter has been redacted. This chapter describes different methods of catalyst preparation and determines the optimum parameters for FTS catalysts. This chapter concludes with experimental results.

Chapter 4

High Thermal Conductive Catalyst support (Modified Catalyst)

4.1 Introduction

Catalysts play an important role in the FTS. However, the turnover rate of the FTS catalyst does not only depend on the dispersion of the catalyst over the support. It also depends on the interplay between the diffusion, reaction, and conversion processes, which occur between catalyst pellets and reactors. The most significant reaction-diffusion coupling mechanisms in the FTS are (1) diffusion-limited product removal from catalyst pellets and reactors, and (2) diffusion-limited reactant arrival at catalytic sites [54]. According to Iglesia et al. (1995), the diffusion-limited product removal from catalyst pellets and reactors leads to enhancing the reabsorption of the α-olefins, a higher molecular weight product, and paraffin when the pellet size or the active size increase. However, diffusion-limited reactant arrival at catalyst sites has less effect when the CO concentration at the catalyst site is low. In this case, the reaction will favor the formation of the light product and decrease C_{5+} selectivity. In order to obtain higher C_{5+} selectivity, the intermediate level of transport restriction is required.

In the fixed bed reactor, large pellets are required to maintain the pressure gradient, and active pellets are required to minimize the size of the reactor to be able to obtain the designed conversion. These requirements lead to the transport restriction in many FTS applications. Using a pellet diameter less than 0.2 mm helps to avoid the transport restriction condition and reaction rate in FTS [55]. Despite that, the heat conductivity is not improved because of the void from the support porosity working as the insulator. High thermal conductivity of support helps to maintain a uniform temperature profile of the synthesis. The low thermal conductivity of the oxide support leads to the hot spot formation within the catalyst bed and causes a non-uniform temperature gradient [55]. The non-

uniform temperature gradient and the hot spot in the catalyst bed can damage the catalyst by reducing its active phase, which causes the deactivation of the FTS catalyst and the creation of methane.

A variety of methods have been introduced to improve the catalytic material performance by increasing the heat and mass transfer so that the catalyst can deliver sufficient reaction enthalpies and reactant species to the reaction site and not limit conversion or selectivity of the reaction under high space velocity conditions [56]. Modified catalyst supports help to improve the gas conversion during the synthesis and/or improve the heat conductivity of the synthesis system. Carbon support, such as carbine, activated carbon, carbon sphere, and carbon nanotube; monolith and metallic foam; egg-shell or core-shell; and metal composite support are used in the FTS in order to improve the overall efficiency of the system [57] [58] [59].

4.1.1 Carbon Support

One reason carbon is used to improve the properties of the catalyst support is its chemical inertness, meaning it does not react during the reaction. In addition, carbon it is available in many forms, such as granules, pellets, fibers, foams, monoliths, fabrics, coating. Carbon is less expensive than other catalyst supports. It has a very high porosity, which causes increased surface area, and is stable at high temperatures [58]. Carbon support also helps enhance the heat capacity of the catalyst during the synthesis. The activated carbon, one type of carbon catalyst support, uses carbon because it is cheap and readily available, and it creates an increased surface area that helps disperse the catalyst material over the surface. However, the increased surface area causes a reduction in the average pore diameter of the catalyst support, which leads to more alcohol and CH_4 formation during the synthesis. Carbon nanotubes (CNTs), cylindrical geometry structures with unique mechanical and electronic properties, is an improved type of carbon catalyst support that

is widely used in FTS because of its catalytic effect. With high electrical and thermal conductivity, uniform pore size and distribution, and a high length-to-diameter aspect ratio, CNTs have higher product selectivity than catalyst support used in commercial enterprises [60]. The composite of carbon material, an even more improved version of carbon catalyst support, combines carbon with a nanofiber [61]. The carbon nanofiber shows a significant increase in the system activity and slow deactivation of the catalyst. However, the carbon nanofiber with a small pore diameter favors high selectivity toward CH_4 and increases WGS. On the other hand, the carbon nanofiber with a bigger pore size has a higher catalyst deactivation rate and lower catalytic activity, but a higher selectivity toward C_{5+}.

4.1.2 Monolith and Metallic Foam Catalyst Support

The monolith catalyst support is developed from the metallic honeycombs, which helps improve the catalytic process. The honeycomb support has a relatively large volume fraction, which reduces heat transfer inside the honeycomb unit. The heat transfer depends on the channel shape and void fraction, and the material properties of the catalyst support structure [62]. The monolith catalyst support acts as the heat exchanger inside the catalyst bed and turns the fixed bed reactor into the heat exchanger type reactor [63]. Instead of metallic honeycombs, the monolith catalyst support is developed from metallic foam, which is then coated with the catalytic material. The monolith catalyst support uniformly distributes the Co particles over the support [63]. When the heat and mass transfer and diffusional restrictions of hydrocarbon are reduced, the C_{5+} selectivity is increased while the CH_4 selectivity and WGS reaction are decreased. The metallic coated foam catalyst support was developed to overcome the limitations in heat and mass transfer in the FT system. With a high heat and mass transfer, the reaction can convert the gas into products more quickly. In fact, a high conversion rate of gas can be obtained from the reactor with

a limited temperature gradient when using the metallic coated foam catalyst support, even more so than when using the monolith catalyst support.

4.1.3 Eggshell or Core-Shell Catalyst Support

Eggshell or core-shell catalyst support was developed to improve selectivity and the rate of the reaction toward C_{5+} in the middle distillates range of hydrocarbon. The thickness variation of the core-shell is the key indicator of the hydrocarbon selectivity [64]. In addition, the core-shell catalyst support is used in the FTS in order to avoid diffusion restriction during the reaction, since the fixed-bed reactor requires large catalyst pellets to maintain a uniform pressure gradient during the synthesis. Both the impregnation and pretreatment methods lead to the nonuniform distribution of the metal catalyst particles, and the high metal concentration at the catalyst support outer surface increases the FTS reaction because most of the reaction happens at the catalyst surface [54]. One type of core-shell catalyst was developed using the traditional catalyst support. However, instead of the support being completely impregnated by the cobalt solution, one benefit of the core-shell is that only the outer surface of the catalyst support is impregnated with cobalt. This thin layer of cobalt on the outer surface showed the improvement of C_{5+} productivity and selectivity because the thin reaction layer reduces the transport restriction. Since it is more difficult for CO than H_2 to diffuse into the catalyst pellet, more methane is produced [54]. Once the cobalt is layered on the outer surface of the catalyst, CO does not need to penetrate the catalyst layers, which increases the selectivity of C_{5+}. Therefore, this type of core-shell catalyst was developed because the range of hydrocarbon can be easily controlled when using it, for example, light isoparaffin.

The second type of core-shell catalyst, the tandem catalyst, uses different layers of materials. The inner layer is the regular FT catalyst and is encapsulated with a layer of zeolite (H-ZSM-5) support to convert the product to the desired range of hydrocarbon.

Zeolite is a catalyst suitable for hydrocracking and isomerization because of its acidic properties. The high metal-surface interaction between zeolite and Co reduces the CO conversion during the synthesis. Thus, the tandem catalyst is the most effective way to convert the reactant gas into hydrocarbon because the reaction between the two surfaces is independent. The hydrocarbon is generated at the core part of the catalyst. Once it leaves the core site, the hydrocarbon reacts with the zeolite layer and turns into the desired product from the isomerization and hydrocracking character of the zeolite and forms long chains of hydrocarbon. However, the second reaction at the zeolite layer is not guaranteed since the short distance between the two surfaces can help the hydrocarbon escape the catalyst without a second reaction [65].

The third type of core-shell catalyst was developed by combining the first two types of core-shell catalysts because it is assumed that the FTS reactions occur only at the surface of the catalyst, making the core of the catalyst unnecessary. Therefore, the core part of the catalyst is substituted with a solid material, for example, glass, and metal, in order to reduce the diffusion restriction of the gasses, reduce the unreacted catalyst inside the core, and improve the heat transfer inside the fixed bed reactor [57]. The core-shell catalyst with the metal core is suitable for an exothermic reaction inside the fixed bed reactor of the FTS. The metal at the catalyst core can gradually dissipate the heat from the exothermic reaction evenly over the catalyst bed even though it may suddenly increase. Hot spots probably will not happen and the reaction can continue inside the reactor because the catalyst has a lower chance to deactivate. The control of temperature results in less methane production and more C_{5+} [57] [66].

4.1.4 High Thermal Conductive Catalyst Support

Thermal conductivity of a catalyst pellet is a function of macropore volume or pellet density [67]. A change in pellet density does not affect micropores inside catalyst pellets

or surface availability of the catalytic reaction. Therefore, the effectiveness of the interior surface of a catalyst pellet during a reaction is strongly dependent upon the resistance to mass and energy transfer through the macropores [68]. Masanune and Smith physically modified the catalyst support in order to improve its heat conductivity properties. They introduced a metal additive to the support material, which improved the capability of the catalyst support to conduct the reaction heat generated during the synthesis.

Metal additive materials such as Cu, Al, stainless steel (SS), Ni, and zinc (Zn), are used to increase the heat transfer rate and isothermal temperature of the catalyst bed of the FTS reactor. However, not all of the metal can used as an additive for the modified catalyst because the metal additive material has to be physically and chemically stable enough during the synthesis to be able to manage the high temperature. For example, Ni and SS are types of metal additive material that are not stable during the FTS. As Ni reacts with synthesis gas, the catalyst support loses Ni particles, which become nickel carbonyl volatile that later reforms down stream. Stainless steel is an opposite; it is stable during synthesis; however, it loses its thermal conductivity properties at high synthesis temperatures.

Unlike stainless steel and Ni, though, Cu is a stable metal additive material for FTS because it does not react during synthesis. Therefore, Sheng et al. used a metal microfiber entrapped catalyst (MFEC) with Cu fiber to increase the heat and mass transfer in a fixed bed reactor [59]. The MFEC with Cu fiber showed significant improvement of temperature distribution inside the catalyst bed as well as improved product selectivity. In addition, this MFEC with Cu fiber significantly improved the radial effective thermal conductivity, to about 50 times higher than traditional alumina support [59]. Likewise, Asalieva et al. mixed Cu powder with the catalyst support to increase heat and mass transfer in a fixed bed reactor. For them, the Cu particles in the catalyst support reacted with the synthesis gas, thus

limiting productivity of the catalyst. In addition, their catalyst support mixed with Cu powder showed a lower pore volume, thus limiting the heat and mass transfer and leading to low productivity and selectivity of the catalyst [69].

Catalyst support can be modified to improve the catalytic performance of the FTS system by increasing productivity and selectivity of the synthesis. To do so, heat conductivity materials can be introduced into the catalyst support to increase the heat transfer. This is especially relevant in fixed bed reactors because they normally have higher CH_4 selectivity than other types of reactors. Table 4-1 summarizes different types of modified catalysts and their thermal conductive materials [70].

Table 4-1 Catalyst support with different modifications

Catalyst type	Material		Catalyst size	Ref
	Support	Conductive		
Core-shell pellet	SiO_2	N/A	2.2 mm	[54]
Core-shell	Al_2O_3	Al	<25μm	[56]
CNFs (cabon nanofibers)	Ni/SiO_2	N/A	2μm	[61]
MFEC (metal microfibrous entrapped catalyst)	Ɣ- Al_2O_3	Cu, SS, or Al	Φ15.9 mm (disk shape)	[59]
Tandem catalyst	SiO_2/H-ZSM-5	N/A	0.85-1.7 mm	[63]
Core-shell/bimodal	SiO_2/ZSM	N/A	0.25-0.85 mm	[65]
Metalic foam	Al_2O_3	Ni	Φ 22 mm, h=1.4mm	[71]
High conductivity pellet	H-Beta zeolite	Al, Cu, or Zn	2.2-2.5x2.5-3.0 mm	[69]
Core shell	Al_2O_3	Al	0.18-0.25 mm	[57]
Monolith	Al_2O_3	Al alloy	Φ 16 mm, h=30mm	[72]

4.2 Thermal Conductivity Measurement

The porous material (SiO_2, Al_2O_3, and TiO_2) can be used as a catalyst support material for the FTS because it provides a large surface area that enhances the synthesis reaction [68]. Therefore, the porosity of the catalyst support works as heat insulation; it

causes a large temperature gradient inside the catalyst bed. This large temperature gradient increases the temperature at the center of the reactor while the temperature at the surface remains low. Hence, the catalyst material for reactors should be designed with thermal conductive properties in mind, especially for fixed-bed reactors.

4.2.1 Heat Transfer

Heat is energy that transfers from a higher temperature to a lower temperature. Heat is generated from the vibration or electronic state of microscopic material. Conductive heat transfer, heat transfer in a solid or a static fluid, is the only mode of heat transfer considered in this experiment. The interaction between the heat flow and temperature field can be explained using the Fourier's law;

$$\vec{q}_{cond} = -k\nabla T$$

where $\vec{q}_{cond}$ is the heat flux

k is the thermal conductivity

∇T is the temperature gradient (a vector normal to the surface)

Heat flux is the rate of heat transfer through a given surface. The ability of heat transfer through a surface depends on the materials and properties of the surface [73].

4.2.2 Inverse Heat Transfer Problem

An inverse analysis is a process that uses a known characteristic value, the effect, to determine an unknown of a physical system, the cause. In this type of analysis, the effect is an observed or measured response of the system, while the cause usually refers to system boundary conditions, initial conditions, thermal properties, internal heat sources, or geometry. In the inverse analysis, the observed effect is used to determine the cause relationship [74].

In this experiment, numerical inverse analysis is used to predict properties of heat generating material by measuring temperature at an outer boundary. In addition, the Semi-Analytical Complex Variable Method (CVSAM) was used to enhance the accuracy and efficiency of the method, which is beneficial in determining the reliability of a system [75] [76] [77]. The thermal conductivity of the traditional and modified SiO_2 catalyst support with the highest productivity were analyzed using CVSAM at different heat loads to monitor improvements in heat transfer.

4.2.3 Experiment Setup

In this experimental setup, a 750 W cartridge heater (ϕ = 3/8" and 3" long) was inserted into the center of a copper tube (ϕd = 1", 1/32" in wall thickness, and 7" in length). Four K-type thermocouples were attached to the heater surface with 3/4" spacing between each to measure the heat generated by the heater. The heater was secured at the center of the copper tube using special fixtures and a mineral wool thermal insulator at both ends to create an annular gap between the copper tube and heater. The annular space created was filled with the catalyst support material. Similar to the heater, four K-type thermocouples were also attached to the outside wall of the copper tube with 3/4" spacing matching the thermocouples inside (Figure 4.1a). All of the thermocouples were connected to a NI-921110-channel via NI cDAQ 9174 (4-slot USB, National Instrument) for data acquisition. The temperature signal from the 8 thermocouples was monitored and recorded using LabVIEW (National Instrument). The copper tube packed with catalyst support was placed horizontally inside an enclosed (2x1x1 ft) plastic box (Figure 4.1b). The plastic box was used to eliminate disturbance and promote the natural convection taking place inside the box. The heater was connected to a 120V/10A power supply (VSP12010 programmable, BK Precision).

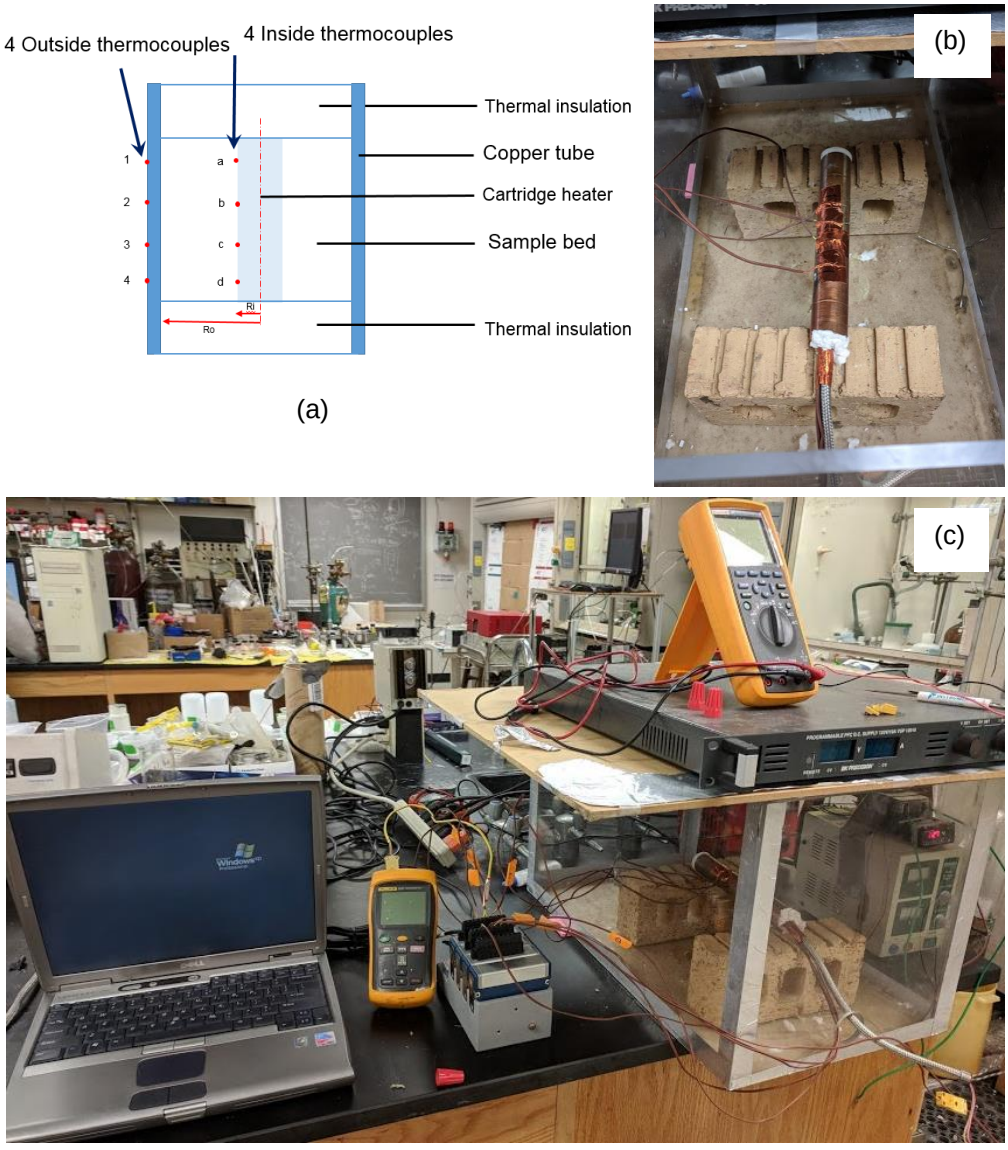

Figure 4-1 Bulk thermal conductive experimental setup a) experimental setup schematic diagram, b) copper tube setup inside enclosed plastic box, and c) experimental setup with power supply and data acquisition.

4.2.4 Experimental Procedure

The catalyst support, packed in between the copper tube and heater, was tested for its thermal conductivity. After the copper tube was packed, it was placed horizontally inside the enclosed plastic box. 1, 2, 3, and 3.4 W of power were supplied to the heater to test the thermal conductivity of catalyst support at different heat loads. The temperature profiles at the heater and copper surfaces were recorded using LabVIEW. Power was supplied to the heater until the temperature of heater and copper tube reached a steady state. Then, the power was cut out. Finally, the data collected in the experiment was analyzed using the inverse analysis method [70] [71] [72].

4.3 Modified Catalyst Preparation (Material and Method)

3 mm SiO_2 support from Saint-Gobain was used for the modified catalyst support in this paper. For improved catalytic performance, SiO_2 catalyst support requires optimum thermal conductivity, pore size (mesopores) and pore volume, a large surface area, a high crush strength, and a high stability during synthesis. However, traditional SiO_2 catalyst support has low heat conductivity because the SiO_2 material and spherical shape of the pores work mostly as a heat insulator. Because of this low heat conductivity, the high temperatures from FTS exothermic reactions are not well dissipated and create hot spots. These hot spots shift the FTS products toward undesired gasses and reduces the activity of the catalyst through sintering of cobalt particles until the catalyst is deactivated. For this reason, in this experiment, thermal conductivity materials, Cu, Al, and graphite rods, were added to the SiO_2 catalyst support to help increase its conductivity properties.

All of the modified catalysts used in this experiment were made of 3 mm cylindrical commercial SiO_2 support. The conductive material was inserted into the center of a

support. After the conductive material was inserted into the catalyst support, the conductive material should have the same length as the catalyst support material(Figure 4-2).

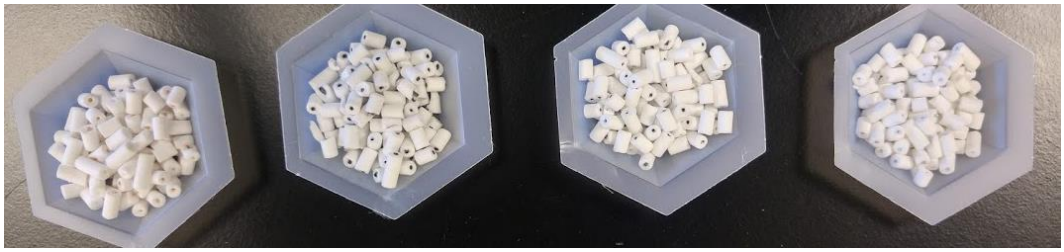

Figure 4-2 SiO_2 catalyst support with different heat conductive materials

(From left to right: copper, 0.9mm graphite rod, 0.7mm graphite rod, and aluminum).

In this experiment, four different types of conductive material were used to conduct the heat for SiO_2 support: copper rod, 0.9 mm graphite rod, 0.7 mm graphite rod, and aluminum rod.

4.3.1 Catalyst Preparation

This section has been redacted.

Chapter 5

Modified Catalyst

This chapter discusses and compares the FTS procedures and results from the four modified SiO_2 catalyst supports against the traditional catalyst support. The modified SiO_2 catalyst supports were created by adding heat conductive material to the center of a SiO_2 support pellet to help dissipate the heat generated during the FTS synthesis experiment. The modified SiO_2 catalyst support was impregnated with design catalyst. The experimental conditions that yielded the highest catalytic performance as seen in Chapter 3 were used to test the pre-catalysts. Finally, inverse analysis was used to determine the overall heat conductivity of the highest performing catalyst.

Figure 5-1 Fischer-Tropsch synthesis experimental setup with condenser unit and graduate flask liquid collector (2nd design)

5.1 Experimental Setup

The FTS experimental setup described in this chapter is similar to the experimental setup described in Chapter 3; however, the liquid collector was modified. In the previous experimental setup, the liquid products were collected under pressure at 300 psig in the gas-liquid separation unit and liquid collector vessel. Because the liquid products from the synthesis cannot be analyzed under this pressure, their oil selectivity, carbon number composition, and aqueous phase were determined only after the synthesis was complete. In this setup, the gas-liquid separation unit and liquid collector vessel were replaced by a water chill condenser graduated flask collector that allowed liquid products to condense at low pressure (0 psig). The water chilled condenser column connected to the top of the graduated flask collector was added to increase the condensation of liquid products and noncondensable products exhausted from the top of the condenser. Hence, the liquid products could be collected and analyzed during the synthesis (Figure 5-1). After the exhausted gas was dried in a desiccant bed as shown in Figure 5.2, the flow rate was measured by a flowmeter (FMA 4000, Omega) and the composition of exhausted gas was analyzed by GC (SRI 8610C, TCD detector with Shin Carbon column from SRI Instruments).

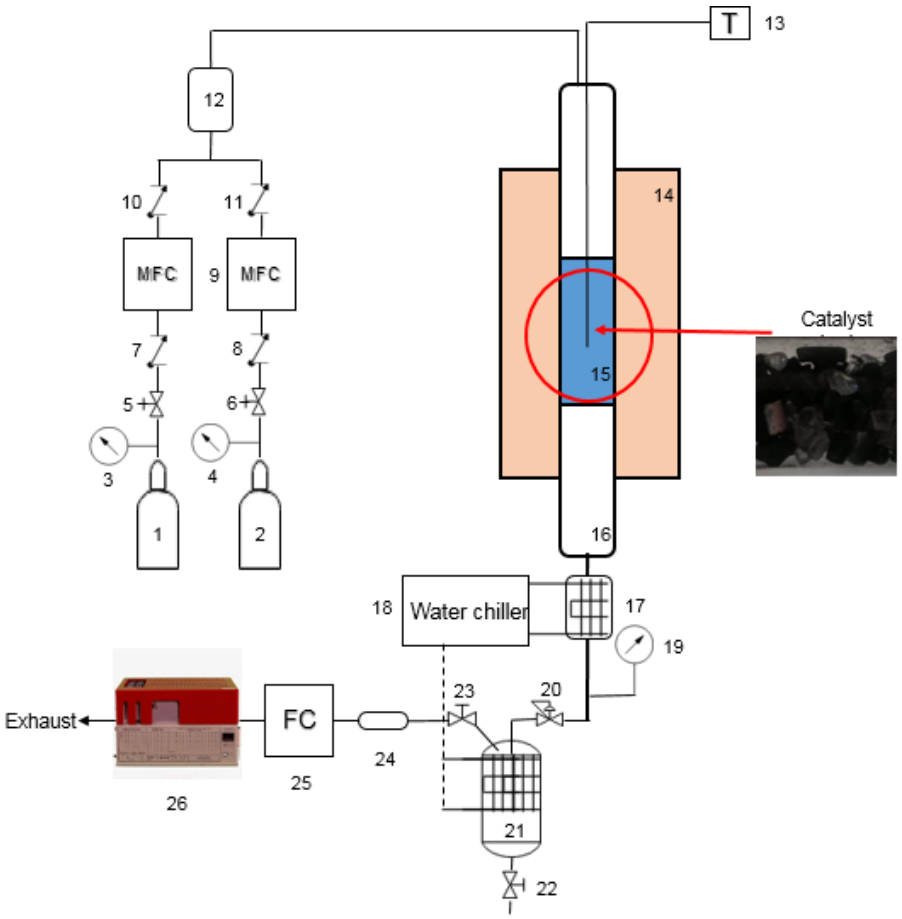

Figure 5-2 Schematic diagram of Fischer-Tropsch synthesis setup 2nd edition

1: CO gas cylinder; 2: H_2 gas cylinder; 3, 4: pressure regulator; 5, 6: gate valve; 7, 8, 10, 11: check valve; 9: mass flow controller; 12: mixing chamber; 13: process thermocouple (catalyst bed); 14: tube furnace; 15: catalyst bed; 16: fixed bed tubular reactor; 17: condenser unit; 18: water chiller; 19: pressure gate; 20: back pressure regulator; 21: water chilled condenser graduated flask liquid collector; 22: drain valve; 23: gas exhaust valve; 24: desiccant bed; 25: flow meter; 26: online GC analysis

5.2 Experimental Procedure

A tubular fixed bed reactor packed with 2 g (base on SiO_2 weight) of pre-catalyst diluted with 2.76 g of quartz chips was used to test the catalytic performance of the FTS. The pre-catalyst was reduced in situ using H_2 at 0 psig with a 100 sccm flow rate. The temperature was increased from room temperature to the desire reduction temperature and maintained at this temperature for 18-20 h. After the pre-catalyst was reduced, the reactor temperature was decreased from reduction temperature to 150°C and maintained there while the system was pressurized at a steady H_2 flow rate of 100 sccm until the pressure reached 300 psig. After the pressure reached the set point, the flow rate of H_2 was reduced to 66.67 sccm and CO was introduced to a system with a 33.33 sccm flow rate. The flow rate between H_2 and CO was kept constant at a ratio of 2:1. Once the flow rate between H_2 and CO was stabilized, the temperature was slowly increased (heating rate 0.6°C/min) to desire temperature, the activation temperature. The temperature, inlet and outlet flow rate, and gas product activity were monitored and recorded at all times during the synthesis.

In a typical experiment, the FTS reactor was continuously run for 5 days before shutting down. During the synthesis, liquid products were collected in a graduated flask collector at 0 psig (Figure 5-3a). The liquid products had two separated layers: the top was the hydrocarbon phase and the bottom was the aqueous phase. The liquid products are normally clear; however, the liquid products collected from the first day of the synthesis were dark because they were mixed with catalyst particles and/or carbon deposition from the previous experiment. The products were collected daily (Figure 5-3b and 5-4) and manually separated. The mass and volume of products were recorded, the hydrocarbon

phase was analyzed using GC (SRI 8610C, TCD detector with a capillary column from SRI Instrument) and the aqueous phase was analyzed using GC-MS (Shimadzu, GC-2010 Plus).

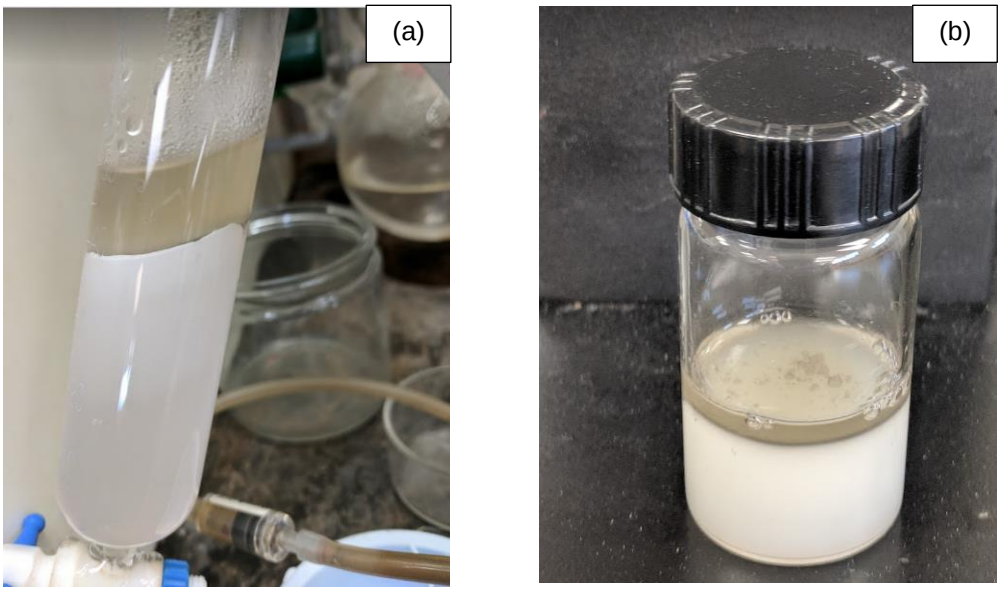

Figure 5-3 Liquid products from FTS experiment (a) liquid products collected in graduated flask collector and (b) liquid products collected from the synthesis: top layer shows hydrocarbon phase and bottom layer shows aqueous phase or water – alcohol mixture.

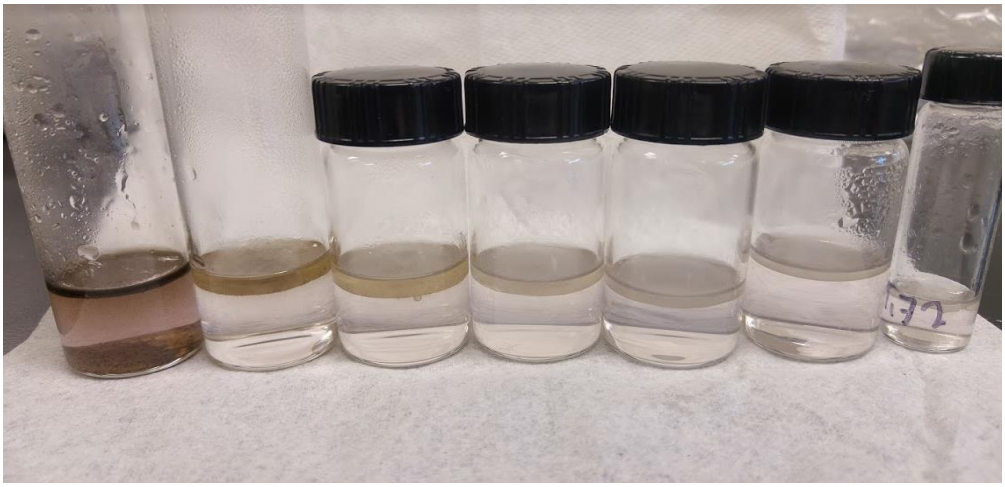

Figure 5-4 FTS liquid products collected during the synthesis. The amount of liquid products (hydrocarbon and aqueous phase) indicated the catalytic performance in each period (from left to right, liquid products from day 1 to day 7)

5.3 Experimental Result and discussion

5.3.1 Catalyst Testing

An FTS catalyst from a traditional catalyst support and a modified SiO_2 catalyst support were run for five days under the same experimental setup and conditions described previously. Table 5-1 shows the summary of products selectivity obtained from the synthesis based on the mass of the products. More specifically, Table 5-1 reports the catalytic productivity, catalyst productivity, percent CH_4 and percent oil selectivity, and percent syngas conversion that were determined from the total collected products and adjusted using a correction factor.

The catalysts used in this FTS experiment resulted in between approximately 20 and 60% syngas conversion. The traditional SiO_2 supported catalyst and the modified SiO_2 catalyst support with an Al core were the most active with a syngas conversion of 49%. The second most active was the modified SiO_2 supported catalyst with 0.9mm graphite

core, and 0.7mm graphite core, which had a syngas conversion between 39 and 43%. The modified SiO_2 supported catalyst with a Cu core had the lowest syngas conversion of 37%. The traditional and modified SiO_2 supported catalyst with and 0.7 mm graphite core had the same percent CH_4 selectivity at 35%; however, the traditional SiO_2 catalyst support show the lowest percent oil selectivity at 8% . Finally, the modified SiO_2 supported catalyst with a Cu core showed the lowest percent CH_4 and the highest percent oil selectivity at 21% and 20%, respectively (Figure 5-5). The hydrocarbon products collected from the experiment were analyzed as previously described, and the results are summarised in Table 5-1.

Table 5-1 The catalytic performance of FTS catalyst on a traditional and a modified catalyst support from new liquid collector setup with a correction factor.

Property	Type of FTS catalyst on					
	Traditional support	Cu core support	Al core support	Graphite 0.7mm core support	Graphite 0.9mm core support	Hollow cylinder
Product:						
Oil, g.	18.2 ± 1.3	23.3 ± 2.1	13.2 ± 0.9	16.2 ± 3.5	20.6 ± 5.0	13.3 ± 2.4
Aqueous phase, g	103.5 ± 15.1	73.0 ± 7.4	106.0 ± 47.2	89.8 ± 21.6	88.5 ± 21.6	58.6 ± 4.3
Wax, g	0.7 ± 0.7	2 ± 1.7	0.9 ± 0.9	0.9 ± 0.4	0.4 ± 0.4	3.1 ± 0.6
Catalytic performance:						
Productivity, mg_{oil}/cm^3-h	36 ± 1	48 ± 3	25 ± 0	29 ± 7	39 ± 7	26 ± 0
CH_4 selectivity, wt%	35 ± 3	21 ± 1	36 ± 4	35 ± 2	32 ± 0	29 ± 3
Oil selectivity, wt%	8 ± 3	20 ± 1	9 ± 4	11 ± 2	13 ± 0	16 ± 3
Syngas conversion, wt%	49 ± 7	37 ± 1	49 ± 21	39 ± 3	43 ± 8	25 ± 4
Oil product distribution:						
Maximum carbon number	$C_{34\pm6}$	$C_{29\pm2}$	$C_{31\pm3}$	$C_{31\pm1}$	$C_{28\pm1}$	$C_{28\pm5}$
Isomer, wt%	7 ± 3	7 ± 3	6 ± 0	8 ± 1	8 ± 3	5 ± 1
n-product (paraffins), wt%	78 ± 2	90 ± 1	89 ± 1	91 ± 2	90 ± 2	93 ± 1
Olefin, wt%	16 ± 5	4 ± 2	6 ± 1	1 ± 1	3 ± 1	3 ± 1
Chain growth, α	0.86	0.88	0.89	0.89	0.86	0.90

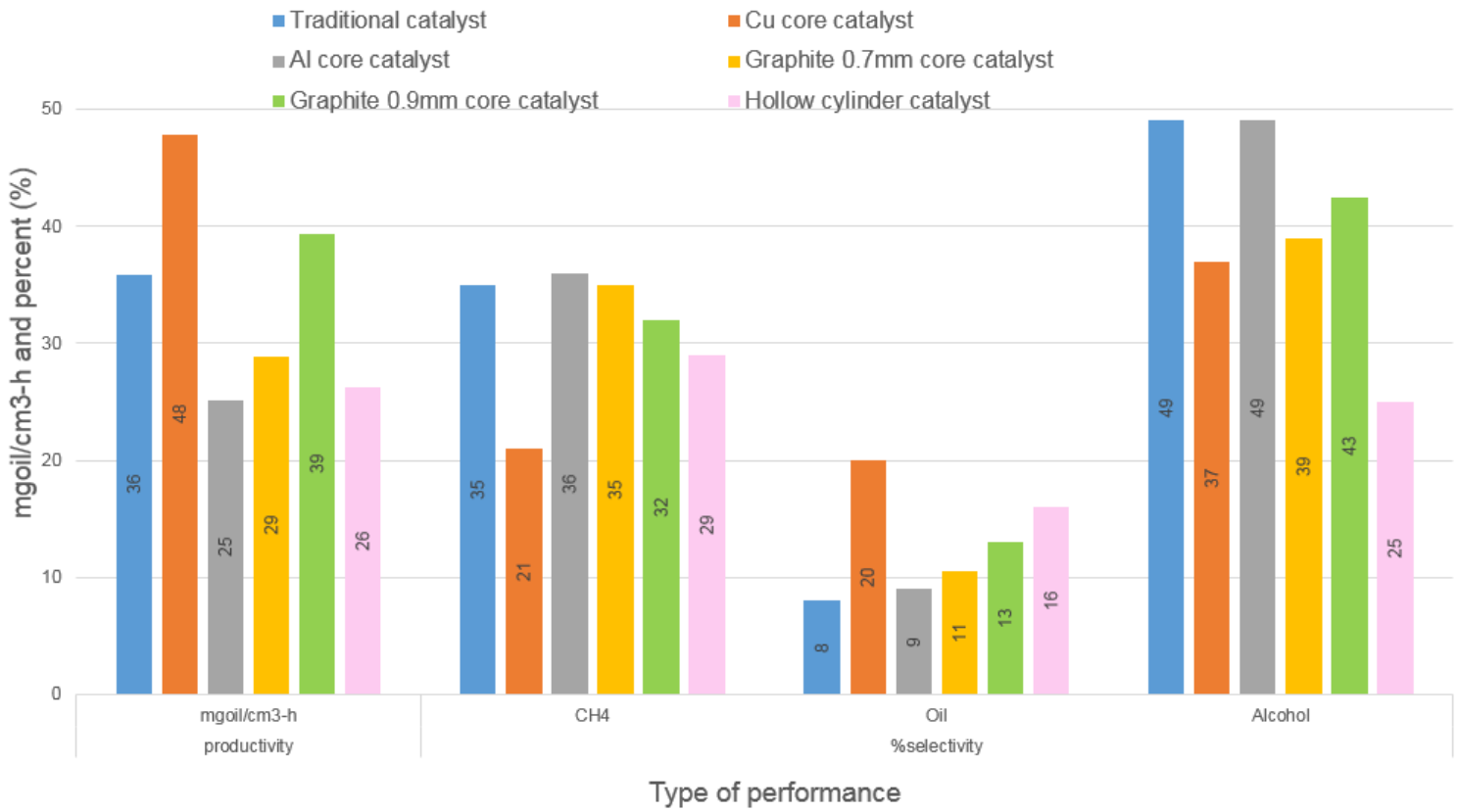

Figure 5-5 Catalytic performance of FTS catalyst on traditional and different modified catalyst support

A reference catalyst, a traditional SiO_2 supported catalyst, which did not contain any thermal conductive material, had a relatively high percent syngas conversion and percent CH_4 selectivity at 32% and 54%, respectively. However, the reference catalyst showed a moderate result in catalyst productivity and percent oil selectivity. In addition, the hydrocarbon products analysis showed it had approximately 10% by mass of both olefin and isomer content.

The introduction of a Cu core as a thermal conductive material affected the catalytic performance: catalyst productivity and percent oil selectivity were highest and percent CH_4 was lowest at 48 mg_{oil}/cm^3-h, 20%, and 21 %, respectively. A modified SiO_2 supported catalyst with a Cu core also improved the hydrocarbon content by reducing olefin content from 16% to 4%. In addition, adding the Cu increased the total mass of the oil product but reduced the aqueous phase product when compared with other supported catalysts at the same synthesis conditions. However, the Cu core had double the amount of wax productivity than the traditional SiO_2 supported catalyst. The benefits of using Cu as a catalyst support core has been explained by Sheng et al.: a Cu core helps manage the exothermic temperature inside a catalyst bed [59], which results in high catalytic selectivity toward C_{5+} and a decrease of the olefin content in the oil product [69].

The introduction of 0.9 mm graphite core as a thermal conductive material had fewer positive effects than the Cu core. The catalyst productivity was slightly increased from 36 mg_{oil}/cm^3-h in a traditional SiO_2 supported catalyst to 39 mg_{oil}/cm^3-h, and the total weight of the oil product increased from 18.2 to 20.6 g by adding the 0.9 mm graphite core. In addition, adding the 0.9 mm graphite resulted in less olefin content, 3%, in the oil product. None of the other types of catalytic performance were improved.

Finally, the introduction of Al and a 0.7 mm. graphite core as a thermal conductive material had no positive effects on the FTS when compared with a traditional SiO_2

supported catalyst. Both of these modified SiO_2 supported catalysts showed lower catalyst productivity but a similar amount of syngas conversion and percent oil and percent CH_4 selectivity when compared with a traditional SiO_2 supported catalyst.

However, the synthesis results of the modified catlayst support with an Al core reported here conflict with Wang et al. For them, the catalyst support with Al additive increased the product selectivity toward C_{5+} but decreased CH_4 and CO_2 selectivity [57]. In addition, for this experiment, the catalyt with the 0.9 mm graphite core had a higher rate of heat and mass transfer than the 0.7 mm graphite core catalyst, resulting in increased productivity toward C_5+ and lower CH_4 selectivity. This agrees with the results of Gardezi et al., who explained that the this increased productivity and lower selectivity was due to the decreased thickness of catalyst support with the 0.9 mm graphite core [64].

The amounts of carbon numbers from the oil product made from FTS catalyst with different catalyst supports were plotted following the ASF distribution law [78]. Table 5-1 shows the chain growth probability (α) of the oil products from the experimental results. According to the α values, the chain growth probability of the oil products obtained from the experimental was between 0.85-0.95, which is in the normal product distribution range for Fischer-Tropsch synthesis [79] [80].

According to these results, the modified SiO_2 supported catalyst with a Cu core had the highest catalytic performance because of the core-shell catalyst effect [57] [54]. For this reason, an aqueous phase product of this catalyst was analyzed for its alcohol content using GC-MS (Shimadzu, GC-2010 Plus). This alcohol content was then compared with the alcohol content from the reference catalyst. The results of tests on the overall thermal conductivity of both the reference and the modified SiO_2 supported catalyst with a Cu core will be discussed in the next section (5.3.2 Bulk Heat Transfer Test).

In the experimental setup with the reference catalyst, the liquid products were collected at 300 psig in a condenser unit and gas-liquid separation unit and liquid collector vessel. However, with the modified SiO_2 supported catalysts, the liquid products were collected at 0 psig in a water chilled condenser graduated flask collector. This was done to increase the ability to track the liquid products on a daily basis, and it resulted in less liquid products through condensation loss as compared to the reference catalyst setup even though a water chilled condenser column was added to increase condensation of products. This condensation loss is due to a different vapor phase ratio that changes at different condensation pressures according to the DePriester Chart [81]. Condensation conditions at lower pressures require lower temperatures and larger condenser surface areas in order to condense the same amount of liquid product, and this was seen in this experiment when the condensation pressure was changed from 300 psig in a condenser unit and gas-liquid separation unit and liquid collector vessel to 0 psig in a water chilled condenser graduated flask collector.

Next, the reference catalyst was used to collect liquid products at 0 psig in a water chilled condenser graduated flask collector. The liquid products from both setups using the reference catalyst were analyzed using GC (SRI 8160C, FID detector with a capillary column from SRI Instrument) and compared against each other, as shown in Figure 5-6. Even after adding a water chilled condenser column, the % mass oil concentration from C_5 to C_9 was significantly less when run at 0 psig as compared to 300 psig. For this reason, a correction factor (see Appendix A) was determined after adjusting the oil concentration and amount of oil collected from these two setups. The correction factor was used to adjust the amount of oil, the ratio of the aqueous phase, and other catalytic productivity of the traditional SiO_2 supported catalyst and the modified SiO_2 supported catalyst with a Cu core (Table 5-2).

Table 5-2 Original and adjusted number of oil production from FTS catalyst on traditional and modified SiO_2 catalyst support in a new and old liquid collector.

Property	FTS catalyst				
	Traditional			Modified –Cu core	
	Old liquid collector	New liquid collector		New liquid collector	
		Original	Adjusted	Original	Adjusted
Product:					
Oil, g.	19.5	4.7	18.2	7.3	23.3
Aqueous phase, g	96.9	56.8	103.5	39.9	73
Wax, g	0	0.7	0.7	2	2
Alcohol, wt%	3.5	13	13	15	15
Catalytic performance:					
Productivity, mg_{oil}/cm^3-h	34	12	36	20	48
CH_4 selectivity, wt%	34	38	35	29	21
Oil selectivity, wt%	11	5	8	13	20
Alcohol selectivity, wt%	1	7	7	9	9
Syngas conversion, wt%	43	30	49	21	37
Productivity, $mg_{oil,alc}/cm^3$-h	40	27	39	32	76
Oil product distribution:					
Maximum carbon number	C_{39}	C_{28}	C_{28}	C_{36}	C_{36}
Isomer, wt%	4	9	13	2	5
n-product (paraffins), wt%	76	80	77	91	91
Olefin, wt%	20	11	10	7	4

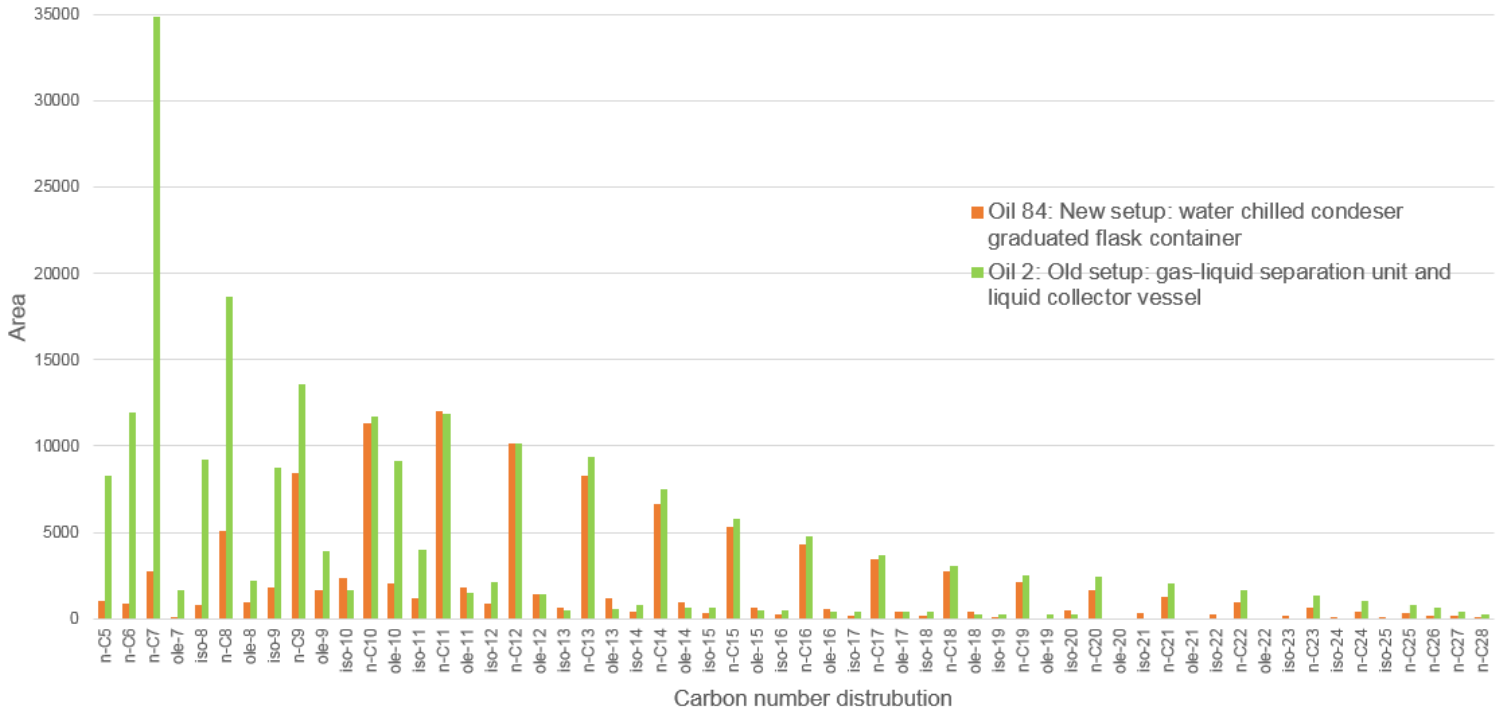

Figure 5-6 Gas chromatogram result of oil products from FTS catalyst on traditional SiO_2 catalyst support at different liquid collector unit setup.

After the liquid products were adjusted, the catalyst productivity of the traditional SiO_2 supported catalyst was increased from 12 mg_{oil}/cm^3-h to 36 mg_{oil}/cm^3-h, % oil selectivity increased from 5% to 8%, and % syngas conversion increased from 30% to 49%. The aqueous phase product collected and analyzed using GC-MS showed about 13% mixed alcohol content, which helped reduce % CH_4 selectivity to about 35% from 38%. Thus, by adding this 13% alcohol selectivity, the overall productivity of the traditional SiO_2 supported catalyst increased to 39 $mg_{oil\text{-}alcohol}/cm^3$-h.

The catalyst productivity, %oil selectivity, and % syngas conversion of a modified SiO_2 supported catalyst with Cu core was as well increased to 48 mg_{oil}/cm^3-h, 20%, and 37% after corrected. %alcohol content in aqueous phase product collected from this catalyst was higher than a traditional SiO_2 supported catalyst about 2% which decreased %CH_4 selectivity to 21%. The mixed alcohol content also increased overall catalyst productivity from 32 $mg_{oil\text{-}alcohol}/cm^3$-h to 76 $mg_{oil\text{-}alcohol}/cm^3$-h. The catalytic activity of the modified SiO_2 catalyst support was improved (increased catalyst productivity and oil selectivity, and reduced CH_4 selectivity) because the heat and mass transfer restrictions were minimized by the Cu core. At a shorter gas traveling distance (from catalyst surface to the Cu core instead of to the center of the SiO_2 pellet), the CH_4 selectivity was significantly reduced, similar to the results from Iglesia et al. [54] and Boa and Tsubaki [65]. In addition, Boa and Tsubaki showed that the core-shell catalyst increased the amount of paraffins when compared with the regular catalyst pellet, which was also seen in this experiment.

5.3.2 Bulk Heat Transfer Test

The traditional SiO_2 supported catalyst and the modified SiO_2 supported catalyst with Cu core, which showed the highest catalytic performance of all catalysts used in this synthesis, were then tested to determine bulk thermal conductivity. Both catalysts were packed identically in-between a copper tube and a heater and tested under the experimental setup and conditions as shown in Figure 5-7. The data obtained from this experiment was analyzed using the numerical inverse problem (Table 5-3).

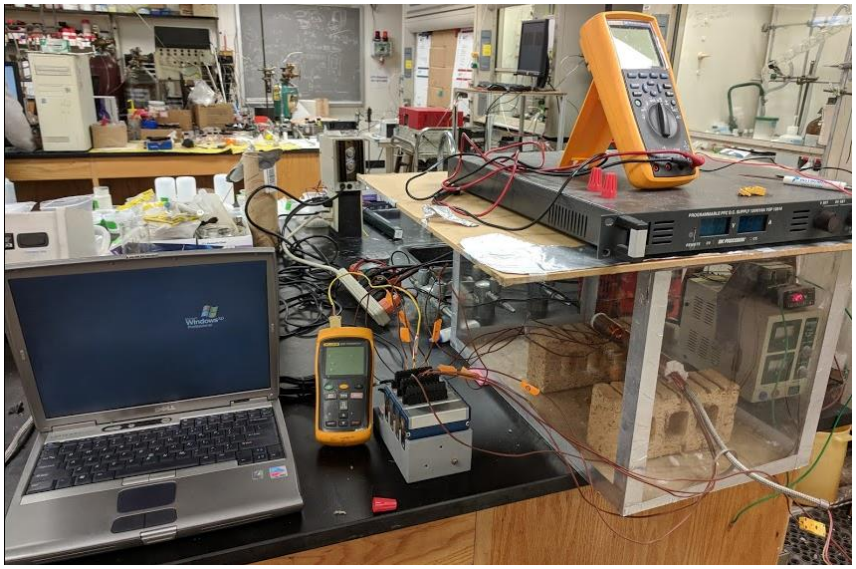

Figure 5-7 Bulk thermal conductivity experimental setup

Table 5-3 Bulk thermal conductivity of traditional SiO_2 catalyst support and modified SiO_2 catalyst support with Cu core at a different power input

Power supply (W)	Traditional SiO_2 catalyst support (3mm pellet)			SiO_2 modified catalyst support with Cu core (3mm pellet)		
	Bulk thermal conductivity (W/m-k)	Temperature (°C)		Bulk thermal Conductivity (W/m-k)	Temperature (°C)	
		Heater surface	Cu tube surface		Heater surface	Cu tube surface
1 W	0.095	65.9	36.5	0.100	64.0	36.8
2 W	0.151	86.7	42.4	0.152	92.0	44.2
3 W	0.134	110.8	48.0	0.150	106.1	47.7
3.4 W	0.125	128.5	53.2	0.140	125.5	53.3
Average	0.126±0.020			0.136±0.021		

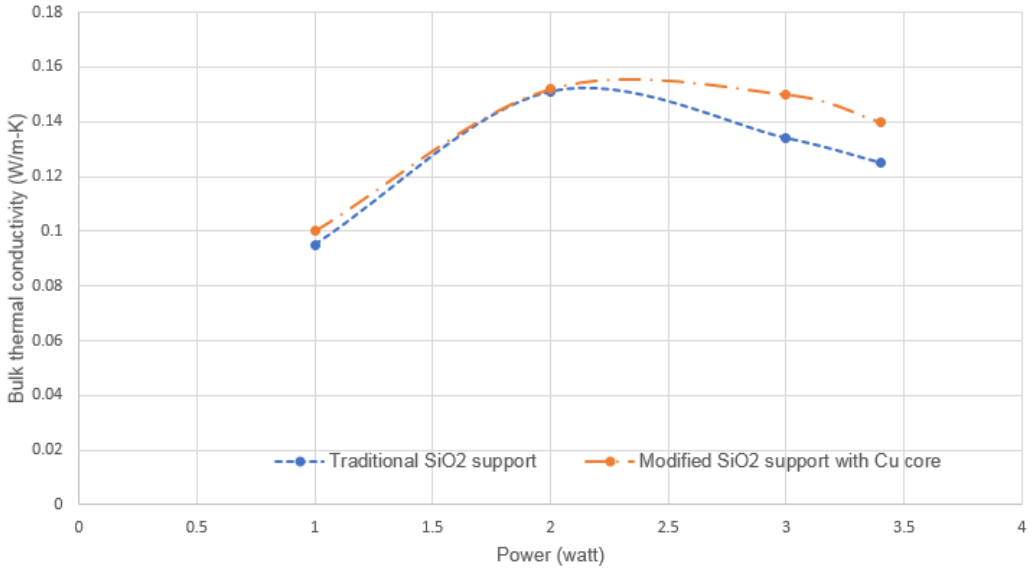

Figure 5-8 Bulk thermal conductivity (W/m-K) between traditional and modified SiO_2 catalyst support at different power input (W).

The results obtained from the numerical inverse heat transfer (Table 5-3) can be plotted as shown in Figure 5-8. This plot shows a small deviation of thermal conductivity between these two catalyst supports at higher power inputs (3 and 3.4W). The results also show that because the catalyst support still had a thick oxide layer, the Cu core in the modified SiO_2 catalyst support did not significantly improve the overall thermal conductivity of the catalyst support, nor did it improve the heat transfer in the catalyst bed, which was also seen in the paper by [57]. Thus, the improvement in catalytic performance of the modified SiO_2 catalyst support with a Cu core might be attributed to other factors, such as surface reactions and the thermal capacity of the catalyst support.

One possible reason for the improvement in catalytic performance of the modified SiO_2 catalyst support with a Cu core is surface reactions. In the modified SiO_2 catalyst support, a Cu core replaced the traditional SiO_2 core, decreasing the traveling distance of the reactant gas, which reduced mass transfer restriction, causing reduced CH_4 selectivity and increased surface reactions of the catalyst. Because of this reason, to better explain the increase in catalytic performance of the modified SiO_2 catalyst support with a Cu core, a hollow cylinder SiO_2 supported catalyst, made of traditional SiO_2 catalyst support with 0.7 mm hole drilled through, was used to test for an increase in surface reactions. According to the experimental results of FTS (Table 5-1), the hollow cylinder SiO_2 supported catalyst did not improve the catalytic performance as compared to the traditional SiO_2 catalyst support, except for a small reduction in % CH_4 selectivity. However, the hollow cylinder SiO_2 supported catalyst should have a higher catalytic performance than the traditional catalyst if surface reactions dominate the synthesis. This is one reason to suspect surface reactions did not improve the catalytic performance of the modified SiO_2 catalyst support with a Cu core.

In addition, because this hollow cylinder SiO_2 supported catalyst can not store heat, any increase in the difference between the furnace temperature and the reactor temperature would indicate that this catalyst has no heat capacity effect at the same level of catalytic performance. Therefore, the furnace and reactor temperatures of the modified SiO_2 catalyst support with Cu core and a hollow cylinder SiO_2 supported catalyst were plotted and compared to see the effect of surface reaction on temperatures.

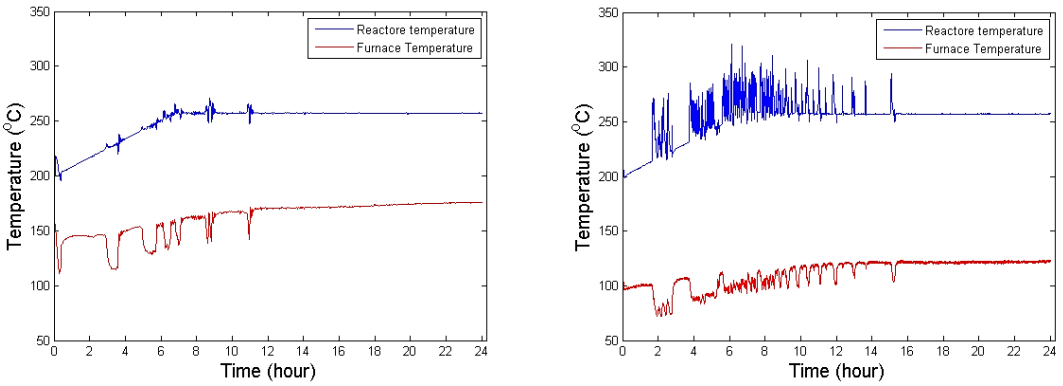

(a) (b)

Figure 5-9 Reaction and furnace temperature as a function of time of a) the modified SiO_2 supported catalyst with a Cu core and b) a hollow cylinder SiO_2 supported catalyst

From the graphs in Figure 5-9, the hollow cylinder SiO_2 supported catalyst showed high fluctuations in reactor temperature in the first 15 h. and a significant temperature difference between the furnace and reactor temperatures; however, the Cu core had small fluctuations in reactor temperature, and the difference between the furnace and reactor temperatures was less than for the hollow cylinder SiO_2 supported catalyst. This is another reason to suspect surface reactions did not improve the catalytic performance of the modified SiO_2 catalyst support with a Cu core.

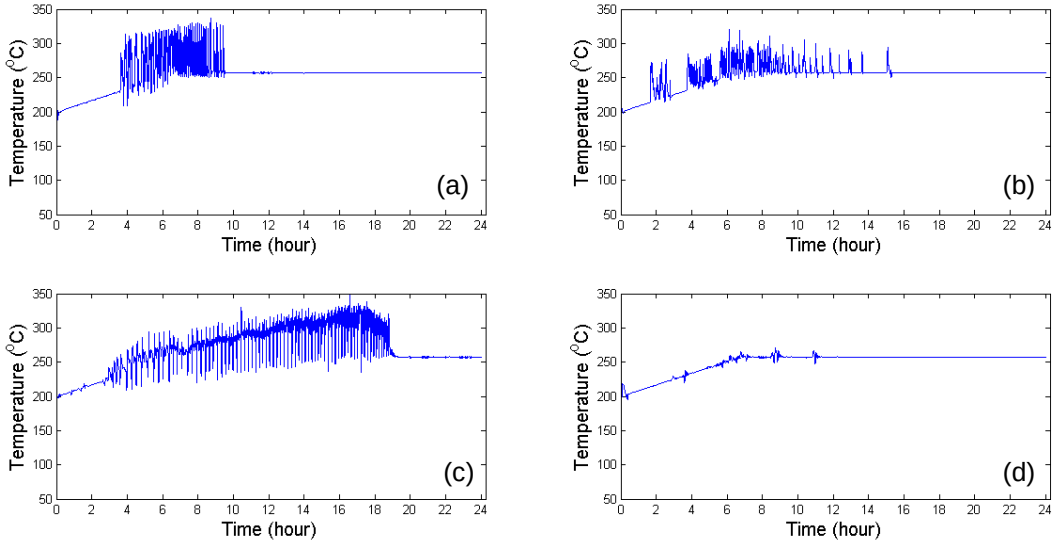

Figure 5-10 Reaction temperature as a function of time of a) the traditional SiO_2 supported catalyst, b) the hollow cylinder SiO_2 supported catalyst, c) the modified SiO_2 supported catalyst with a 0.9 mm graphite core, and d) the modified SiO_2 supported catalyst with a Cu core

Next, to determine the heat capacity effect on the synthesis, the reactor temperatures obtained from the FTS of the traditional catalyst, the modified catalyst with a Cu core and 0.9 mm graphite core, and the hollow cylinder catalyst were plotted and compared (Figure 5-10). Per the results, reactor temperatures for all of the catalysts studied started to stabilize around 15 h after the synthesis started. In addition, the traditional catalyst (38°C), the modified catalyst with a 0.9 mm graphite core (43°C), and the hollow cylinder catalyst (35°C) showed high fluctuations in reactor temperatures after synthesis was activated. However, the modified SiO_2 catalyst support with a Cu core showed only small fluctuations in reactor temperature in the first 15 h. As seen in Figure 5-10, the heat capacity of the Cu core reduced the temperature swing from the 38°C exhibited

by the tradional catalyst support to 5°C. This reactor temperature behaviour of the modified SiO_2 catalyst support with a Cu core is similar to Sheng et al. experimental results using the Cu MFEC; using a Cu core significantly reduces the temperature swing in a packed bed [59]. These experimental results are also supported by a numerical simulation that will be explained in a next section.

5.3.3 Influence of Core-Shell Material Selection on Transient Thermal Performance

The flow patterns in reacting packed media are complex. They vary in space and time due to the evolving chemical reaction. The FT reaction is particularly complex since the reaction involves the generation of a number of products, all with different densities and viscosities. Changing compositions downstream can result in a change in flow path through the media thus further changing the composition of the products. For a very active reaction, the catalyst is sensitive to flow conditions, and this results in an unsteady reaction system. For FTS, this could result in significant temperature swings with time through the catalyst bed. However, a core-shell material composed of a ceramic support layer deposited on a metal core could be considered. The metal core will act as a thermal well to the ceramic support to smooth temperature variations with time. For FTS, this should result in a more uniform reaction product, for example, less methane production.

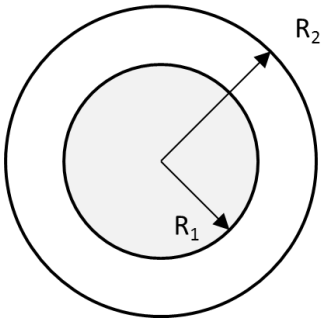

Figure 5-11 A core-shell geometry

This smoothing effect can be illustrated by performing a simple unsteady heat conduction analysis for the core-shell geometry shown in Figure 5-11. The flow of energy via heat conduction is governed by the heat equation:

$$\rho C \frac{\partial T}{\partial t} - \nabla \cdot k \nabla T = Q$$

where T is temperature

C is the specific heat capacity

ρ is the density

k is the thermal conductivity

Q is the volumetric heat source

The volumetric heat source is non-zero in the shell and zero in the core. This mimics the exothermic reaction that occurs in the shell.

The equation was solved numerically for two cases. In the first case, the core and shell are both composed of porous silica. In the second case, the shell is porous silica while the core is copper. The following properties were used.

Material	ρC(J/m^3*K)	k(W/m*K)
Porous Silica	1.61E5	0.14
Copper	3.35E6	400

The heat source was assumed to be a periodic function of time with a frequency of approximately 16 cycles per hour.

R_1, mm	1.0
R_2, mm	1.5
Initial Temperature at t=0s, ^{o}C	250
Q, W/m^3	1.0E6*(1.0+0.2*sin(ω*t))
ω, Hz	0.03

A convection heat flux boundary condition was used (heat coefficient of 10.0 W/K*m^2 and fluid temperature of 230^{o}C). The numerical solutions for both cases are shown in the graph below (Figure 5-12).

The results show a temperature swing of nearly 15^{o}C for the silica core. However, the copper core reduces that swing to approximately 4^{o}C, which is a significant reduction in temperature variation with time. There is also a more gradual transition from the initial temperature to the steady state for the copper core compared to the silica core. These improved results are due to the larger heat capacity and thermal conductivity of the copper core compared to the silica material.

Both the simulation and experimental results showed that adding Cu as a core material help improved the heat capacity of the modified SiO_2 catalyst support by reducing the temperature swing of the experiment and stabilizing the exothermic reactions of the synthesis. These results agree with Sheng et al., who studied a high conductivity catalyst structure for applications in exothermic reactions using Cu fiber MFEC as a catalyst support. They found that the Cu fiber in MFEC significantly reduced the temperature swing from 70 to 10°C during synthesis in a packed bed reactor [59]. The heat capacity from the Cu core was acting as a phase change material that helped stabilized the reaction temperature and improved selectivity [82].

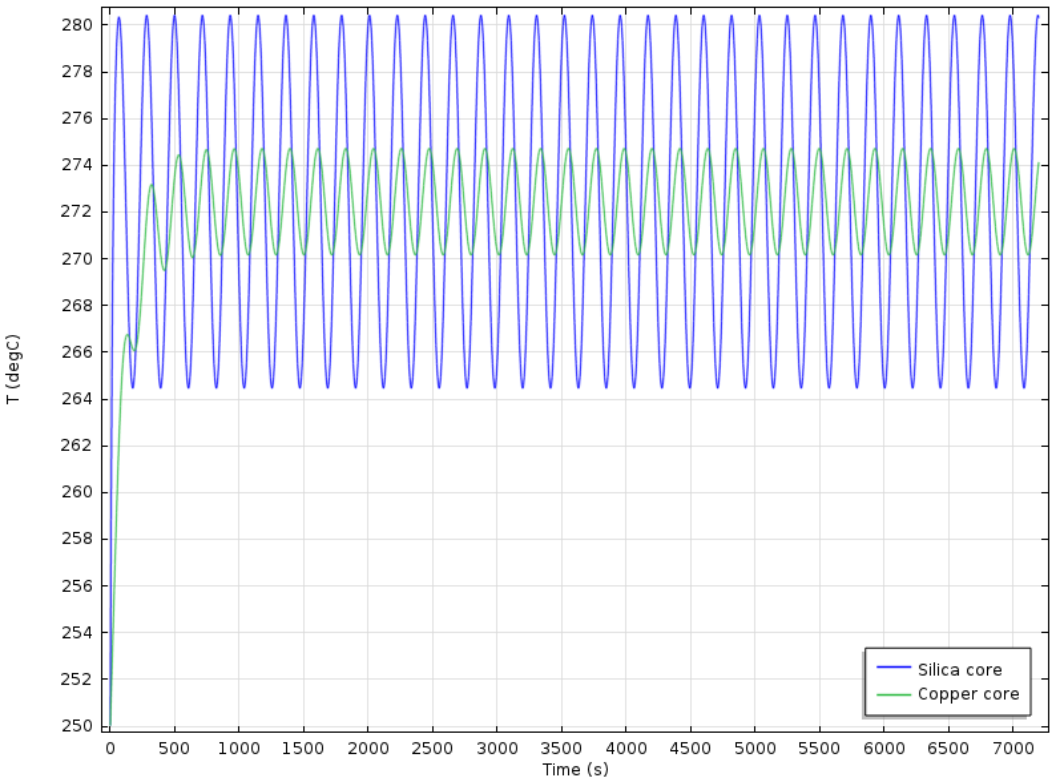

Figure 5-12 A numerical solution of reaction temperature between traditional SiO_2 catalyst support (SiO_2 core) and modified SiO_2 catalyst support (Cu core)

Chapter 6

Conclusion and Future Work

6.1 Conclusion

In this paper, catalytic performance of the FTS is the main concern because even slight changes in preparation or synthesis conditions could affect productivity and selectivity. In order to determine optimum synthesis conditions, the experimental procedure had two main goals: 1) to identify the most effective loading, promotor, drying method, and temperatures, and 2) to find the highest catalytic performance among various modified SiO_2 catalyst supports with different heat conductive materials.

The main results from the parametric study in catalyst preparation (chapter 3) are:

1. The designed catalyst gave the highest catalytic performance.
2. The [redacted] dry method most improved the reduction of the catalyst and most increased catalyst dispersion.
3. The selected precursors gave the highest catalytic performance and stability of catalyst support.
4. The reaction temperature of [redacted] °C was the optimum temperature for increasing oil selectivity and decreasing wax.

Therefore, all of these conditions were used in the catalyst preparation for this experiment. Furthermore, using these conditions resulted in increased catalyst distribution with optimum size and reduction, and decreased agglomeration and sintering, which resulted in higher productivity and selectivity toward long-chain hydrocarbons.

The main results from the modified SiO_2 catalyst support (chapter 4-5) are:

1. The modified SiO_2 catalyst support with a Cu core showed the highest catalytic performance. The modified SiO_2 catalyst support with a Cu core increased catalyst productivity, % oil selectivity, and % alcohol selectivity as compared to the traditional SiO_2 catalyst support. The increases were from 48 to 76 $mg_{oil\text{-}alcohol}/cm^3$-h, from 11% to 20%, and from 10% to 15%, respectively.

2. The modified SiO_2 catalyst support with a Cu core reduced % CH_4 selectivity from 35% to 21%, a 30% decrease, when compared with the traditional SiO_2 catalyst support.

3. The heat capacity of a modified SiO_2 catalyst support was improved after a Cu core was added, resulting in decreased temperature swings and improved synthesis performance.

6.2 Future Work

6.2.1 Improve the thermal conductivity measurement experimental setup and procedure

The thermal conductivity measurement experimental setup can be improved by passing or purging an innert gas before the measurement to eliminate the effect of air from the experiment.

6.2.2 Catalyst characterization of the spent modified SiO_2 catalyst support from the FTS process

The modified SiO_2 supported catalyst with cores of different thermal conductive materials should be analyzed after the synthesis using XRD and TEM to observe the affects of sintering and agglomeration of catalyst particles.

6.2.3 Analyze the catalytic performance of the modified SiO_2 supported catalyst with a Cu core in different size reactors

The modified SiO_2 supported catalyst with a Cu core should be tested in larger reactors (ϕ 1”) to determine how much the reaction effect catalytic performance and the efficiency of the system can improve.

6.2.4 Improve thermal conductivity of catalyst support using a pure graphite or a higher percent graphite content

Graphite is a cheap material with high thermal conductivity (25-470 W/m-k), and it is chemically stable during the FTS. In this paper, the modified SiO_2 supported catalyst showed higher catalyst productivity than a traditional SiO_2 catalyst support but did not improve other types of catalytic activity. One of the reasons the modified SiO_2 supported catalyst did not improve catalytic activity is the low % graphite content of the graphite cores used in this paper. According to AlexZander, when used as a core in a modified catalyst, both 0.7 and 0.9 mm graphite cores have only about 68% graphite content [83]. Therefore, if the core material has higher % graphite content, then the thermal conductivity and heat capacity should be increased, leading to improved catalytic performance of the modified SiO_2 catalyst support.

Appendix A

The oil correction factor for a liquid phase product collected from a water chilled condenser graduated flask collector

The oil correction factor from GC analysis

Carbon number	correction factor	Carbon number	correction factor
n-C5	0.061452615	ole-16	0.684491351
n-C6	0.037057832	iso-17	0.241998377
n-C7	0.039098685	n-C17	0.466791191
ole-7	0.017367522	ole-17	0.55543414
iso-8	0.044090357	iso-18	0.249546702
n-C8	0.137100732	n-C18	0.448587835
ole-8	0.223412323	ole-18	0.667394346
iso-9	0.105182461	iso-19	0.232935938
n-C9	0.311075222	n-C19	0.432626594
ole-9	0.212693245	ole-19	0
iso-10	0.719766869	iso-20	0.833666185
n-C10	0.487182136	n-C20	0.338857787
ole-10	0.112514443	ole-20	0
iso-11	0.147769464	iso-21	0
n-C11	0.510860299	n-C21	0.317784455
ole-11	0.599469246	ole-21	0
iso-12	0.215490834	iso-22	0
n-C12	0.502789452	n-C22	0.29256869
ole-12	0.523521256	ole-22	0
iso-13	0.699528131	iso-23	0
n-C13	0.443963993	n-C23	0.252252064
ole-13	1.084798947	iso-24	0
iso-14	0.282710662	n-C24	0.210187385
n-C14	0.447101771	iso-25	0
ole-14	0.761097941	n-C25	0.204640234
iso-15	0.277028338	n-C26	0.175039587
n-C15	0.466780722	n-C27	0.173407823
ole-15	0.675207193	n-C28	0.208627021
iso-16	0.258315678		
n-C16	0.452414995		

Appendix B

Gas chromatogram of oil from FTS catalyst with different type of modified catalyst support

Gas chromatogram of oil product from FTS catalyst on a tradition catalyst support

at 300 psig

Lab name: SRI Instruments
Client: Valued Customer
Client ID: N2024
Analysis date: 09/25/2014 13:11:23
Method: Syringe Injection
Description: CHANNEL 1
Column: RESTEK 15METER MXT-500
Carrier: HELIUM AT 1 PSI
Data file: Oil 02.ASC (C:\Users\gc\Desktop\ferm\FT oil spring 2014)
Sample: FT Oil 2
Operator: Wan

Temperature program:

Init temp	Hold	Ramp	Final temp
35.00	5.000	10.000	350.00
350.00	50.000	0.000	350.00

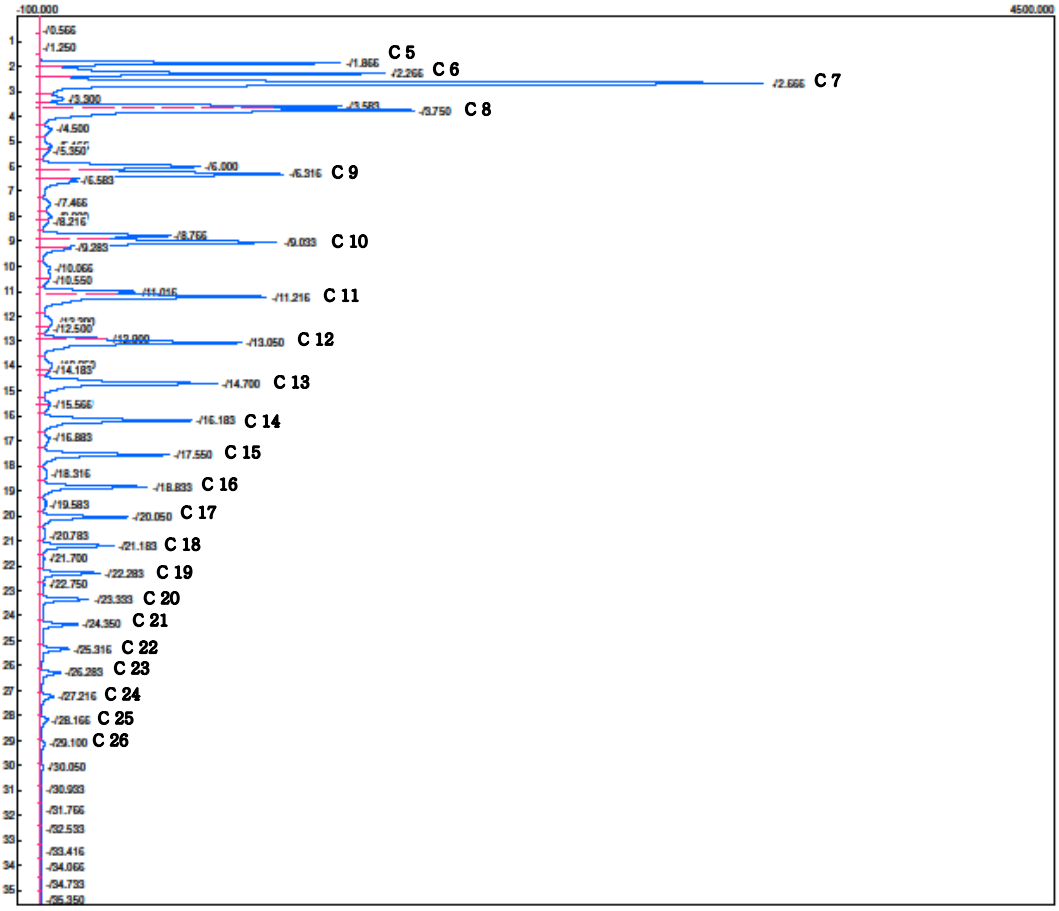

Gas chromatogram of oil product from FTS catalyst on a tradition catalyst support

at 0 psig

Lab name: SRI Instruments
Analysis date: 11/16/2017 15:02:39
Method: Syringe Injection
Description: CHANNEL 1
Column: RESTEK 15METER MXT-1
Carrier: HELIUM AT 1 PSI
Data file: Oil_84 (C:\Users\gc\Desktop\fern\FT oil spring 2014-new)
Sample: FT Oil 84
Operator: Fern
Comments: Ficher-Tropsch synthesis:
Modified catalyst support: Copper core

Temperature program:

Init temp	Hold	Ramp	Final temp
35.00	5.000	10.000	350.00
350.00	5.000	0.000	350.00

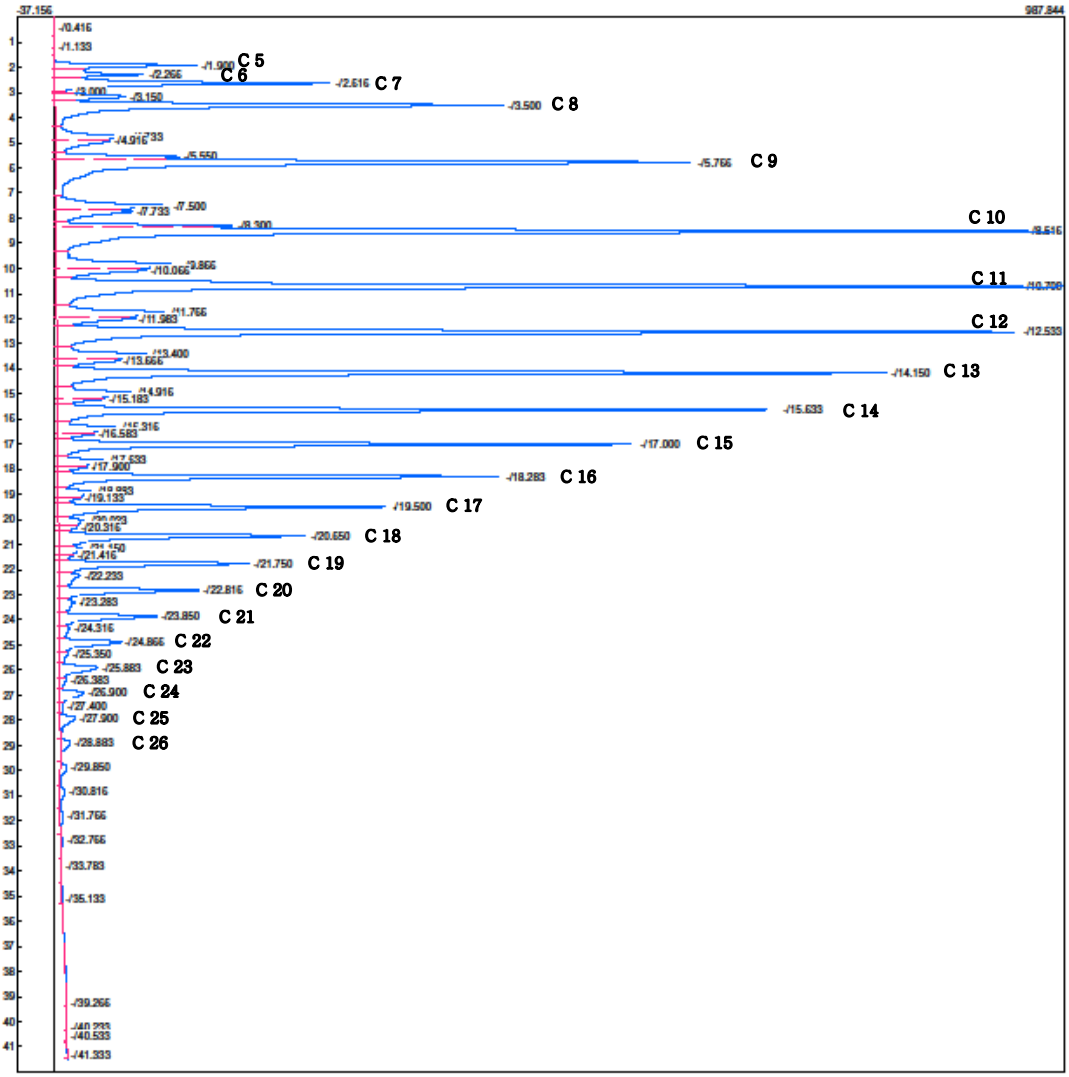

Gas chromatogram of oil product from FTS catalyst on a modified catalyst support with hollow cylinder

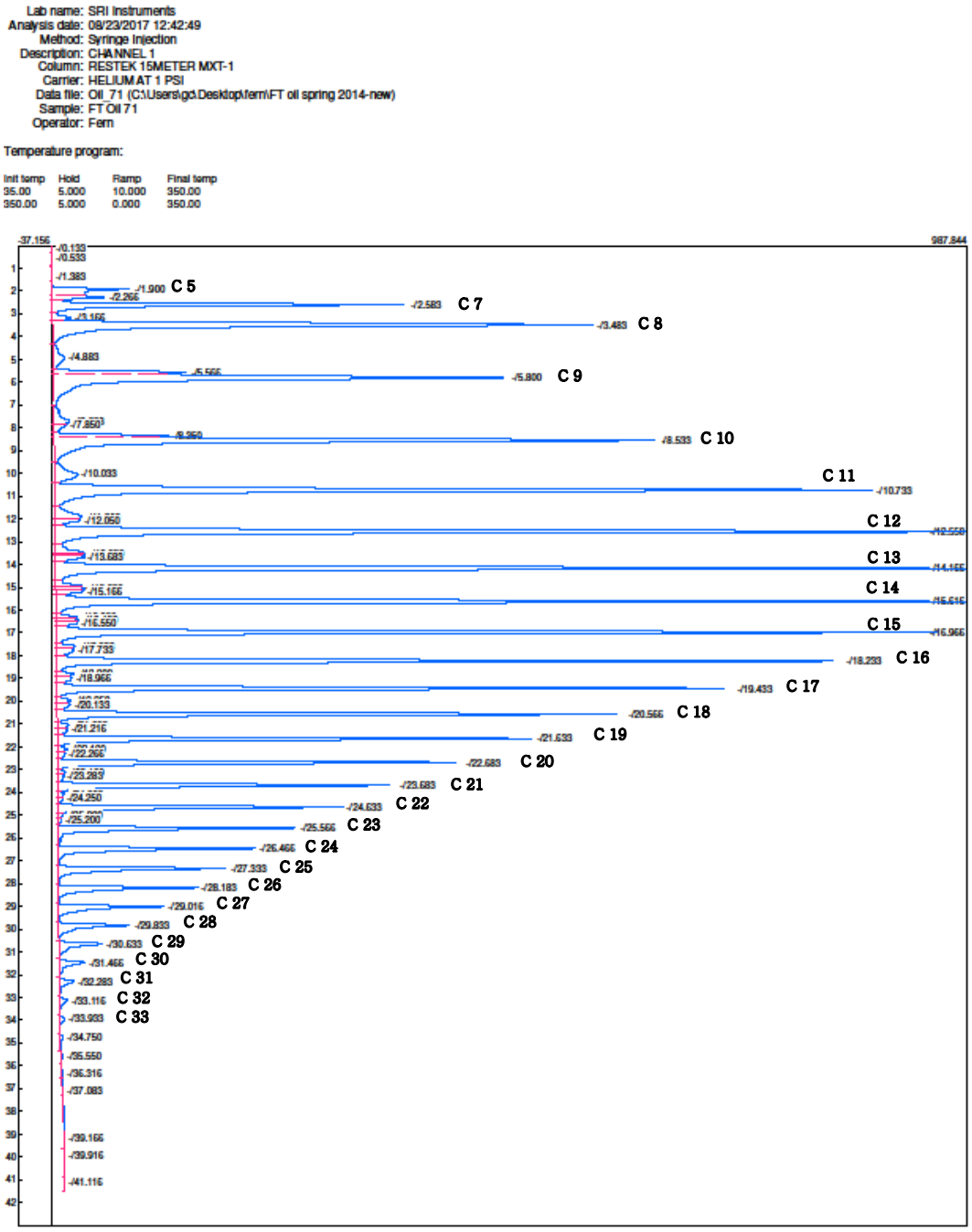

Gas chromatogram of oil product from FTS catalyst on a modified catalyst support with Cu core

Lab name: SRI Instruments
Analysis date: 03/12/2018 10:14:40
Method: Syringe Injection
Description: CHANNEL 1
Column: RESTEK 15METER MXT-1
Carrier: HELIUM AT 1 PSI
Data file: Oil 95 (C:\Users\gc\Desktop\fern\FT oil spring 2014-new)
Sample: Oil 95_1
Operator: Fern

Temperature program:

Init temp	Hold	Ramp	Final temp
35.00	5.000	10.000	350.00
350.00	5.000	0.000	350.00

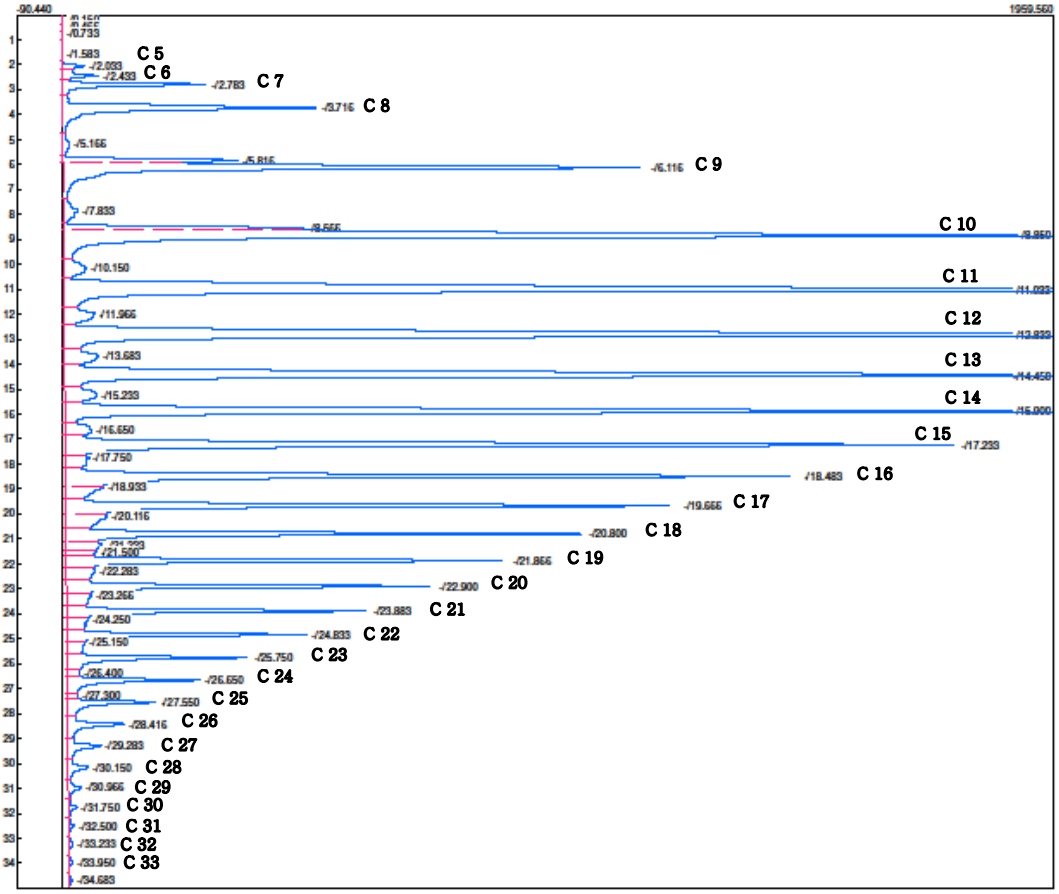

Gas chromatogram of oil product from FTS catalyst on a modified catalyst support with Al core

Lab name: SRI Instruments
Analysis date: 08/23/2017 14:51:54
Method: Syringe Injection
Description: CHANNEL 1
Column: RESTEK 15METER MXT-1
Carrier: HELIUM AT 1 PSI
Data file: Oil_73 (C:\Users\gc\Desktop\fern\FT oil spring 2014-new)
Sample: FT Oil 73
Operator: Fern

Temperature program:

Init temp	Hold	Ramp	Final temp
35.00	5.000	10.000	350.00
350.00	5.000	0.000	350.00

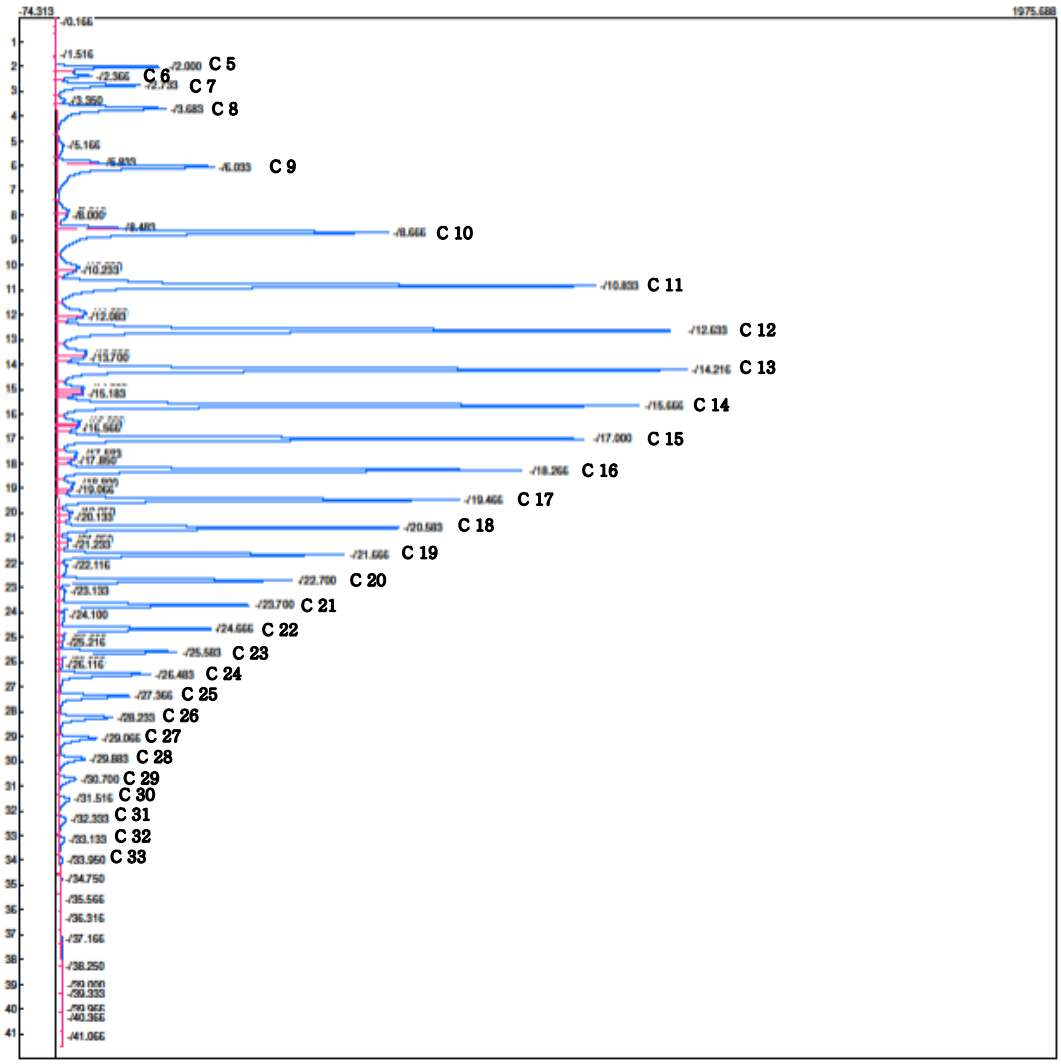

Gas chromatogram of oil product from FTS catalyst on a modified catalyst support with 0.7 mm graphite core

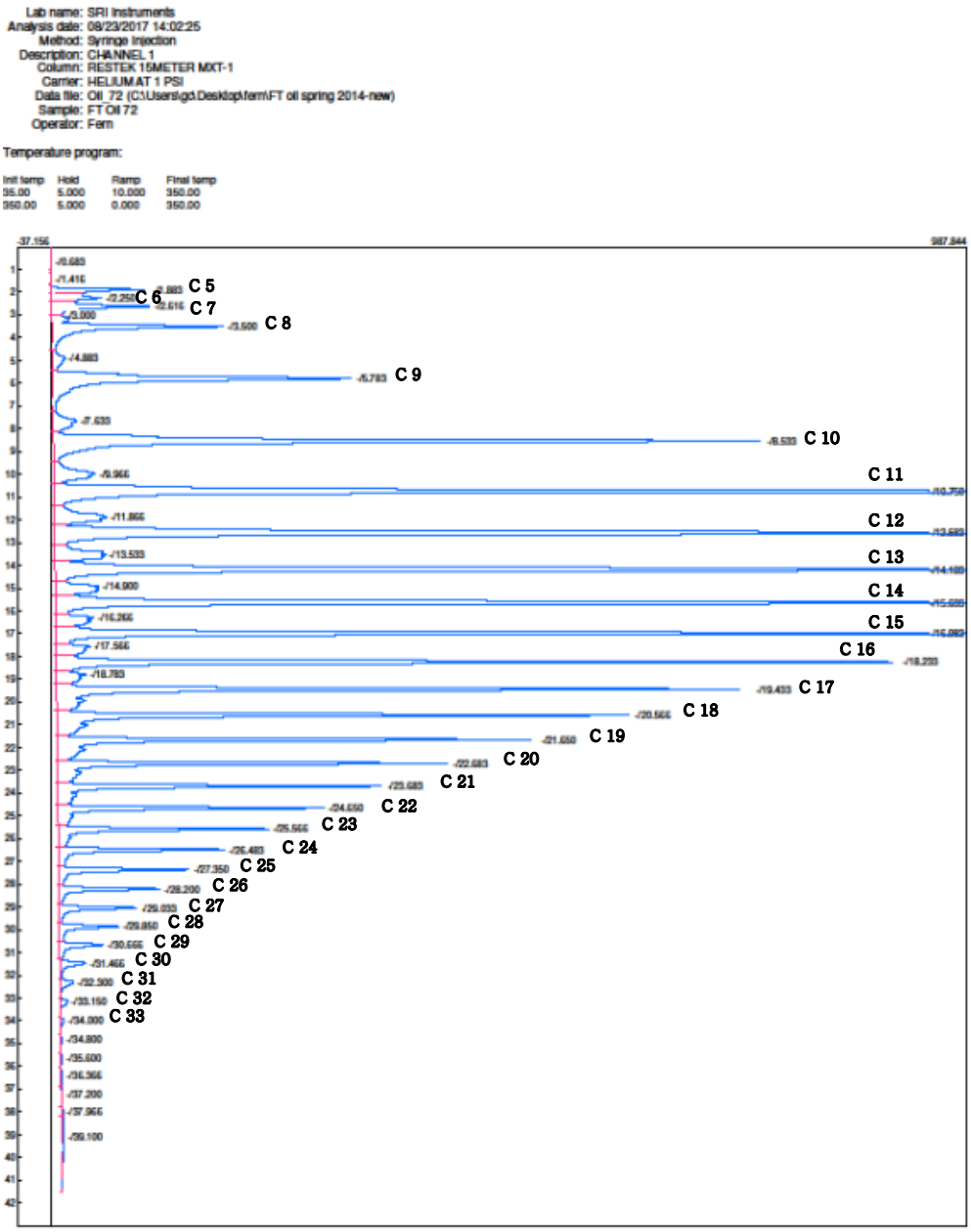

Gas chromatogram of oil product from FTS catalyst on a modified catalyst support with 0.9 mm graphite core

Lab name: SRI Instruments
Analysis date: 08/29/2017 16:08:04
Method: Syringe Injection
Description: CHANNEL 1
Column: RESTEK 15METER MXT-1
Carrier: HELIUM AT 1 PSI
Data file: Oil_75 (C:\Users\gd\Desktop\fern\FT oil spring 2014-new)
Sample: FT Oil 75
Operator: Fern

Temperature program:

Init temp	Hold	Ramp	Final temp
35.00	5.000	10.000	350.00
350.00	5.000	0.000	350.00

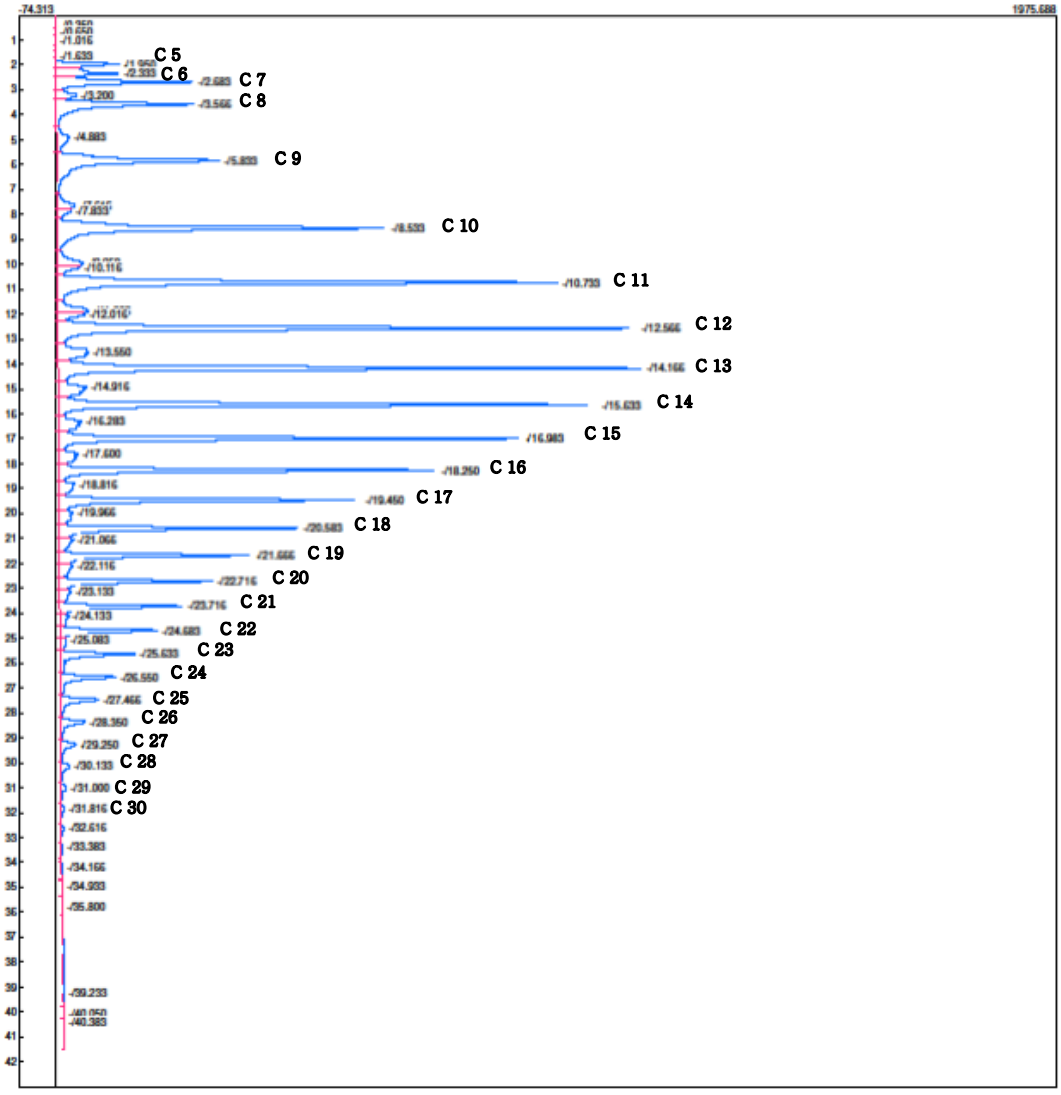

Appendix C

Gas chromatogram of a gas phase products from FTS catalyst

A typical gas chromatogram of a tail gas products from the Fischer-Tropsch Synthesis using FTS catalyst

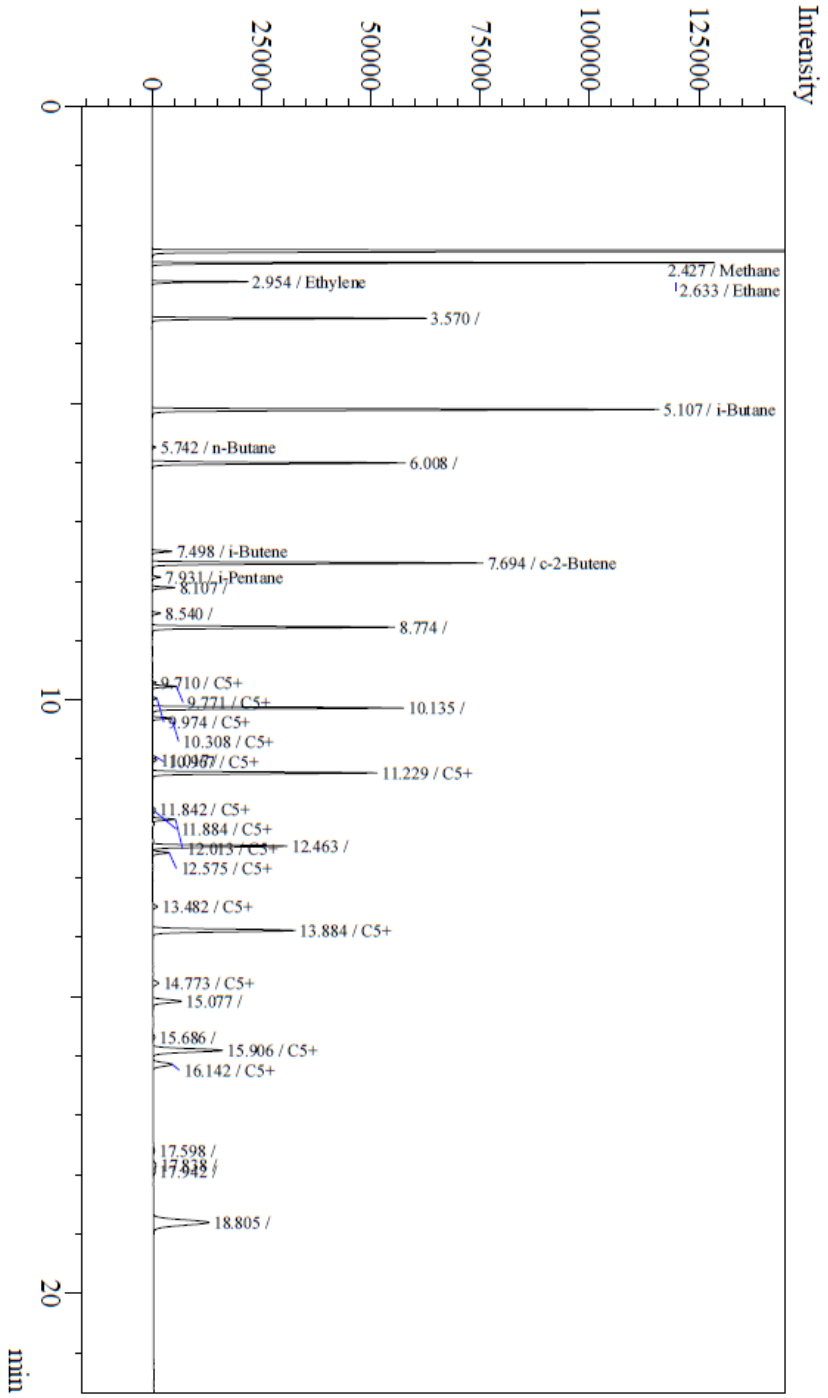

References

[1] "Independent Statistic & Analysis U.S. Energy Information Administration," U.S. Energy Information Administration, 14 September 2017. [Online]. Available: https://www.eia.gov/todayinenergy/detail.php?id=32912. [Accessed 28 March 2018].

[2] S. S. Ail and S. Dasappa, "Biomass to Liquid Transportation Fuel via Fischer-Tropsch Synthesis - Technology review and current scenario," *Renewable and Sustainable Energy Reviews,* vol. 58, pp. 267-286, 2016.

[3] R. B. Anderson, The Fischer-Tropsch Synthesis, CRC Press, 2016.

[4] M. E. Dry, "Fischer-Tropsch synthesis over iron catalyst," *Catalysis Letters,* vol. 7, pp. 241-252, 1990.

[5] M. E. Dry, "Fischer-Tropsch synthesis-Industrial," in *I.T. Horvath (ed.), Encyclopedia of Catalysis, Vol. 3*, N. Y. , USA, Wiley New York, 2003, pp. 347-403.

[6] M. E. Dry, "Chemical concepts used for engineering purposes," in *Studies in Surface Science and Catalysis Fischer-Tropsch Technology*, Elsevier, 2004, pp. 196-257.

[7] S. Sie and R. Krishna, "Fundamentals and selection of advanced Fischer-Tropsch reactors," *Applied Catalysis A: General,* vol. 186, pp. 55-70, 1999.

[8] B. H. Davis, "Fischer-Tropsch synthesis: Overview of reactor development and future potentialities," *Prepr. Pap.-Am. Chem. Soc., Div. Fuel Chem.,* vol. 48, no. 2, pp. 787-790, 2003.

[9] B. H. Davis, "Fischer-Tropsch synthesis: Overview of reactor development and future potentialities," *Topics in Catalysis ,* vol. 32, pp. 143-168, 2005.

[10] M. E. Dry, "The Fischer-Tropsch process: 1950-2000," *Catalysis Today,* vol. 71, pp. 227-241, 2002.

[11] H. Storch, N. Golumbic and R. Anderson, The Fischer-Tropsch and Related Synthesis, New York: John wiley & Sons, 1951.

[12] A. P. Steynberg, M. E. Dry, B. H. Davis and B. B. Breman, "Fischer-Tropsch reactors," in *Fischer-Tropsch Technology*, Elsevier Science & Technology Books, 2004, pp. 64-195.

[13] A. K. Dalai and B. H. Davis, "Fischer-Tropsch synthesis: A review of water effects on the performances of unsupported and supported Co catalyst," *Applied Catalysis A: General,* vol. 348, pp. 1-15, 2008.

[14] G. Jacobs, M. C. Ribeiro, W. Ma, Y. Ji, S. Khalid, P. T. Sumodjo and B. H. Davis, "Group 11 (Cu, Ag, Au) promotion of 15%Co/Al2O3 Fischer-Tropsch synthesis catalysts," *Applied Catalysis A: General,* pp. b137-151, 2009.

[15] J. A. van Bokhoven and J. T. Miller, "d Electron Density and Reactivity of the d Band as a Function of Particle Size in Supported Gold Catalysts," *J. Phys. Chem. C,* pp. 9245-9249, 2007.

[16] H. Al-Megren, H. Chen, Y. Huang, M. AlKinany, P. P. Edwards, T. Xiao and Y. Wang, "TPO/TPD study on the activation of silica supported cobalt catalyst," *Appl Petrochem Res,* vol. 3, pp. 25-34, 2013.

[17] S. Brunauer and P. T. E. Emmett, "Adsorption of Gases in Multimolecular Layers," *J. Am. Chem. Soc.,* vol. 60, no. 2, pp. 309-319, 1938.

[18] B. S. I. Staff, Determine of the Specific Surface Area of Solids by Gas Adsorption. BET Method, B S | Standards, 1910.

[19] S. Brunauer, P. Emmett and E. Teller, "Absorption of Gases in Multimolecular Layers," *Journal of the American Chemical Society,* vol. 60, no. 2, pp. 309-319, 1938.

[20] "Particle Analytical," WordPress , [Online]. Available: http://particle.dk/methods-analytical-laboratory/surface-area-bet-2/. [Accessed 18 April 2018].

[21] Y. Liu, J. Chen, K. Fang, Y. Wang and Y. Sun, "A large proe-size mesoporous zirconia supported cobalt catalyst with good performance in Fischer-Tropsch synthesis," *Catalysis Communication ,* vol. 8, pp. 945-949, 2007.

[22] K. Mahomed, "Thermogravimetric Analysis (TGA) Theory and Application," California, 2016.

[23] A. Gervasini, "Temperature Programmed Reduction/Oxidation (TPR/TPO) Methods," in *Calorimetry and Thermal Methods in Catalysis*, Berlin, Heidelberg, Springer, 2013, pp. 175-195.

[24] O. O. James and S. Maity, "Temperature Programmed Reduction (TPR) Studies of Cobalt Phases in γ-alumina Supported Cobalt Catalyst," *Journal of Petroleum Technology and Alternative Fuels,* pp. 1-12, 2016.

[25] J. Goodge, "Integrating Reserach and Education: Moving Research Result into Geoscience Course," Carleton College, 2016 November 2016. [Online]. Available: https://serc.carleton.edu/research_education/geochemsheets/elementmapping.html . [Accessed 12 December 2017].

[26] S. Swapp, "Geochemical Instrumentation and Analysis," Uinversity of Wyoming, 26 May 2017. [Online]. Available: https://serc.carleton.edu/research_education/geochemsheets/techniques/SEM.html. [Accessed 16 March 2018].

[27] G. J. Hutchings and J. C. Vedrine, "Heterogenous Catalyst Preparation," in *Basic Principles in Applied Catalysis*, Heidelberg, Springer-Verlag, 2004, pp. 217-258.

[28] M. R. Feaviour and E. R. Schofield, "Scientific Bases for the Preparation of Heterogeneous Catalysts: PGMs Feature in Greater Understanding of Precursors and Active Species," *Platinum Metals Rev.,* pp. 42-44, 2007.

[29] J. A. Schwarz, C. Contescu and A. Contescu, "Methods for Preparation of Catalytic Materials," *Chem. Rev.,* pp. 477-510, 1995.

[30] M. Prat, "On the Influence of Pore Shape, Contact Angle and Film Flows on Drying of Capillary Porous Media," *International Journal of Heat and Mass Transfer,* vol. 50, pp. 1455-1468, 2007.

[31] P. Munnik, P. E. de Jongh and K. P. de Jong, "Control and Impact of the Nanoscale Distribution of Supported Cobalt Particles Used in Fischer-Tropsch Catalysis," *J. Am. Chem. Soc.,* pp. 7333-7340, 2014.

[32] C. Perego and P. Villa, "Catalyst Preparation Methods," *Catalysis Today,* pp. 281-305, 1997.

[33] P. Munnik, P. E. de Jongh and K. de Jong, "Recent Developments in the Synthesis of Supported Catalysts," *Chemical Reviews,* pp. 6687-6718, 2015.

[34] S. L. Soled, E. Iglesia, R. A. Fiato, J. E. Basumgartner, H. Vroman and S. Miseo, "Control of Metal Dispersion and Structure by Changes in the Solid-State Chemistry

of Supported Cobalt Fischer-Tropsch Catalysts," *Topics in Catalysis,* pp. 101-109, 2003.

[35] J.-G. Choi, "Reduction of supported cobalt catalysts by hydrogen," *Catalysis Letters,* pp. 291-296, 1995.

[36] A. Zamniyan, Y. Mortazavi, A. A. Khodadadi and A. N. Pour, "Effect of mass transfer limitations on catalyst performance during reduction and carburization of iron based Fischer-Tropsch synthesis catalysts," *Journal of Energy Chemistry,* pp. 795-803, 2013.

[37] A. Saib, M. Claeys and E. van Steen, "Silica Supported Cobalt Fischer-Tropsch Catalysts: Effect of Pore Diameter of Support," *Catalysis Today,* vol. 71, pp. 395-402, 2002.

[38] S. M. Walas, Chemical Process Equipment: Selection and Design, Newton: Butterworth-Heinemann Publishing, 1988.

[39] E. A. Gulbransen and K. F. Andrew, "The Kinetics of the Oxidation of Cobalt," *Journal of the Electrochemical Society,* vol. 98, no. 6, pp. 241-251, 1951.

[40] A. M. Saib, J. L. Gauché, C. J. Weststrate, P. Gibson, J. H. Boshoff and D. J. Moodley, "Fundamental Science of Cobalt Catalyst Oxidation and Reduction Applied to the Development of a Commercial Fischer-Tropsch Regeneration Process," *Industrial & Engineering Chemistry Research,* vol. 53, pp. 1816-1824, 2014.

[41] G. Jacobs, T. K. Das, Y. Zhang, J. Li, G. Racoillet and B. H. Davis, "Fischer–Tropsch synthesis: support, loading, and promoter effects on the reducibility of cobalt catalysts," *Applied Catalysis A: General,* vol. 233, pp. 263-281, 2002.

[42] E. Rytter, N. E. Tsakoumis and A. Holmen, "On the Selectivity to Higher Hydrocarbons in Co-Based Fischer-Tropsch Synthesis," *Catalysis Today,* vol. 261, pp. 3-16, 2016.

[43] A. R. de la Osa, A. Romero, F. Dorado, J. Valverde and P. Sánchez, "Influence of Cobalt Precursor on Efficient Production of Commercial Fuels over FTS Co/SiC Catalyst," *Catalysts,* vol. 98, no. 6, pp. 1-19, 2016.

[44] Ø. Borg, N. Hammer, B. C. Enger, R. Myrstad, O. A. Lindvåg, S. Eri, T. H. Skagseth and E. Rytter, "Effect of Biomass-Derived Synthesis Gas Impurity Elements on Cobalt Fischer-Tropsch Catalyst Performance Including in Situ Sulphur and Nitrogen Addition," *Journal of Catalysis,* vol. 279, no. 1, pp. 163-173, 2011.

[45] K. Cats, J. Andrews, O. Stéphan, K. March, C. Karunakaran, F. Meirer, F. de Groot and B. Wechkhuysen, "Active Phase distribution Changes within a Catalyst Particle during Fischer-Tropsch Synthesis as Revealed by Multi-Scale Microscopy," *Catalysis Science & Technology,* vol. 6, pp. 4438-4449, 2016.

[46] X. Sun, A. I. O. Suarez, M. Meijerink, T. van Deelen, S. Ould-Chikh, J. Zečević, K. P. de Jong, F. Kapteijn and J. Gascon, "Manufacture of Highly Loaded Silica-Supported Cobalt Fischer-Tropsch Catalysts from a Metal Organic Framework," *Nature Communications,* vol. 8, pp. 1-8, 2017.

[47] P. Munnik, P. E. de Jongh and K. P. de Jong, "Control and Impact of the Nanoscale Distribution of Supported Cobalt Particles Used in Fischer-Tropsch Catalysis," *J. Am. Chem. Soc.,* pp. 7333-7340, 2014.

[48] P. Munnik, N. A. Krans, P. E. de Jongh and K. P. de Jong, "Effects of Drying Conditions on the Synthesis of Co/SiO2 and Co/Al2O3 Fischer-Tropsch Catalysts," *ACS Catalysis,* vol. 4, pp. 3219-3226, 2014.

[49] M. K. Albretsen, B. Huang, K. Keyvanloo, B. F. Woodfield, C. H. Bartholomew, M. D. Argyle and W. C. Hecker, "Effect of Drying Temperature on Iron Fischer-Tropsch Catalysts Prepared by Solvent Deficient Precipitation," *Journal of Nanomaterials,* pp. 1-11, 2017.

[50] T. Wang, Y. Ding, Y. Lü, H. Zhu and L. Lin, "Influence of lannthanum on the performance of Zr-Co/activated carbon catalyst in Fischer-Tropsch synthesis," *Journal of Natural Gas Chemistry,* vol. 17, pp. 153-158, 2008.

[51] M. Hmmati, M. Kazemeini, J. Zarkesh and F. Khorasheh, "Effect of lanthanum doping on the lifetime of Co/Ɣ-Al2O3 catalyst in Fischer-Tropsch synthesis," *Journal of the Taiwan Institute of Chemical Engineers,* vol. 43, pp. 704-710, 2012.

[52] W. Ma, G. Jacobs, P. Gao, T. Jermwongratanachai, W. D. Shafer, V. R. R. Pendyala, C. H. Yen, J. L. Klettlinger and B. H. Davis, "Fischer-Tropsch Synthesis: Pore Size and Zr Promotional Effects on the Activity and Selectivity of 25%Co/Al2O3 catalysts," *Applied Catalysis A: General,* vol. 475, pp. 314-324, 2014.

[53] E. S. S. L. Iglesia and R. Fiato, "Fischer-Tropsch Synthesis on Cobalt and Ruthenium Metal Dispersion and Support Effects on REaction Rate and Selectivity," *Journal of Catalysis,* vol. 137, pp. 212-224, 1992.

[54] E. Iglesia, S. L. Soled, J. E. Baumgartner and S. C. Reyes, "Synthesis and Catalytic Properties of Eggshell Cobalt Catalysts for the Fischer-Tropsch Synthesis," *Journal of Catalysis,* pp. 108-122, 1995.

[55] R. J. Madon, E. R. Bucker and W. F. Taylor, "Department of Energy, Final Report, Contract No. E (46-1)-8008," 1977.

[56] H. c. Lee, Y. Potapova and D. Lee, "A core-shell structured, metal-ceramic composite-supported Ru catalyst for methane steam reforming," *Journal of Power Sources,* vol. 216, pp. 256-260, 2012.

[57] D. Wang, C. Chen, J. Wang, L. Jia, B. Hou and D. Li, "High thermal conductive core-shell structured Al2O3@Al composite supported cobalt catalyst for Fischer-Tropsch synthesis," *Applied Catalysis A: General,* vol. 527, pp. 60-71, 2016.

[58] E. Bailón-Garcí, F. J. Maldonado-Hódar, A. F. Pérez-Cadenas and F. Carrasco-Marín, "Catalysts Supported on Carbon Materials for the Selective Hydrogenation of Citral," *Catalysts,* pp. 853-877, 2013.

[59] M. Sheng, H. Yang, D. R. Cahela, W. R. Yantz Jr., C. F. Gonzalez and B. J. Tatarchuk, "High Conductivity Catalyst Structures for Applications in Exothermic Reactions," *Applied Catalysis A: General,* pp. 143-152, 2012.

[60] M. Zaman, A. Khodadi and Y. Mortazavi, "Fischer-Tropsch Synthesis Over Cobalt Dispersed on Carbon Nanotubes-Based Supported and Activated Carbon," *Fuel Processing Technology,* vol. 90, pp. 1214-1219, 2009.

[61] J. A. Díaz, M. Martínez-Fernández, A. Romero and J. L. Valverde, "Synthesis of Carbon Nanofibers Supported Cobalt Catalysts for Fischer-Tropsch Process," *Fuel,* vol. 111, pp. 422-429, 2013.

[62] G. Groppi and E. Tronconi, "Design of novel monolith catalyst supports for gas/solid reactions with heat exchanger," *Chemical Engineering Science,* vol. 55, pp. 2161-2171, 2000.

[63] J.-I. Yang, J. H. Yang, H.-J. Kim, H. C. D. H. Jung and H.-T. Lee, "Highly effective cobalt catalyst for wax production in Fischer-Tropsch synthesis," *Fuel,* vol. 89, pp. 237-243, 2010.

[64] S. A. Gardezi, L. Landrigan, B. Joseph and J. T. Wolan, "Synthesis of Tailored Eggshell Cobalt Catalysts for Fischer-Tropsch Synthesis Using Wet Chemisistry Techniques," *Ind.Eng.Chem.Res,* pp. 1703-1712, 2012.

[65] J. Bao and N. Tsubaki, "Core-Shell Catalysts and Bimodal Catalysts for Fischer-Tropsch Synthesis," *Catalysis,* pp. 216-245, 2012.

[66] L. Fratalocchi, C. G. Visconti, L. Lietti and E. Tronconi, "A Novel Preparation Method for "Small" Eggsehll Co/γ-Al2O3 Catalysts: A Promising Catalytic System ofr Compact Fischer-Tropsch Reactors," *Catalysis Today,* pp. 125-132, 2015.

[67] R. A. Mischke and J. M. Smith, "Thermal Conductivity of Alumina Catalyst pellets," *I & EC Fundamentals,* vol. 4, no. 4, pp. 288-292, 1962.

[68] S. Masanune and J. M. Smith, "Thermal Conductivity of Porous Catalyst Pellets," *Journal of Chemical and Engineering Data,* vol. 8, no. 1, pp. 54-58, 1963.

[69] E. Asalieva, K. Gryaznov, E. Kulchakovskaya, I. Ermolaev, L. Sineva and V. Mordkovich, "Fischer-Tropsch synthesis on cobalt-based catalyst with different thermally conductive additives," *Applied Catalysis A: General,* pp. 260-266, 2015.

[70] C. N. Satterfield, G. A. Huff, H. G. Stenger, J. L. Carter and R. Madon, "A Comparison of Fischer-Tropsch Synthesis in a Fixed Bed Reactor and in a Slurry Reactor," *Ind. Eng. Chem. Fundam,* vol. 24, pp. 450-454, 1985.

[71] J. C. Park, N. S. Roh, H. Chun, H. Jung and J.-I. Yang, "Cobalt Catalyst coated Metallic Foam and Heat-Exchanger Type Reactor for Fischer-Tropsch Synthesis," *Fuel Processing Technology,* vol. 119, pp. 60-66, 2014.

[72] D. Merino, O. Sanz and M. Montes, "Effect of catalyst layer macroporosity in high-thermal-conductivity monolithic Fischer-Tropsch catalyst," *Fuel,* vol. 210, pp. 49-57, 2017.

[73] D. W. Hahn and M. N. Özişik, "Heat Conduction," John Wiley & Sons, Inc., 2012.

[74] F. Chinesta and E. Cueto, "Inverse Analysis," in *PGD-Based Modeling of Materials, Structures and Processes*, Springer, Cham, 2014, pp. 171-189.

[75] S. Patil, S. Chintamani, R. Kumar and B. Dennis, "Determination of orthotropic thermal conductivity in heat generating cylinder," in *ASME 2016 International Mechanical Engineering Congress and Exposition*, Phenix, 2016.

[76] S. Patil, S. Chintamani, J. Grisham, R. Kumar and B. H. Dennis, "Inverse Determination of Temperature Distribution in Partially Cooled Heat Generating Cylinder," in *ASME 2015 International Mechanical Engineering Congress and Exposition*, Houston, 2015.

[77] O. Fabela, S. Patil, S. Chintamani and B. H. Dennis, "Estimation of Effective Thermal Conductivity of Porous Media Utilizing Inverse Heat Transfer Analysis on Cylindrical Configuration," in *ASME 2017 International Mechanical Engineering Congress and Exposition*, Tampa, 2017.

[78] A. Steynberg and M. Dry, Fischer-Tropsch Technology, Elsevier Science & Technology Book, 2004.

[79] A. Tavakoli, M. Sohrabi and A. Kargari, "Application of Anderson-Schulz-Flory (ASF) Equation in the Product Distribution of Slurry Phase FT Synthesis with Nanosized Iron Catalysts," *Chemical Engineering Journal,* vol. 136, no. 2-3, pp. 358-363, 2008.

[80] I. Puskas and R. Hurlbut, "Comments About the Causes of Deviations from the Anderson-Schulz-Flory Distribution of the Fischer-Tropsch Reaction Products," *Catalysis Today,* vol. 84, pp. 99-109, 2003.

[81] E. E. Ludwig, Process Design for Chemical and Petrochemical Plants, Volume 2, Houston: Gulf Professional Publishing, 1994.

[82] A. O. Odunsi, T. S. O'Donovan and D. A. Reay, "Temperature Stabilisation in Fischer-Tropsch Reactors Using Phase Change Material (PCM)," in *4th Micro and Nano Flows Conference*, London, 2014.

[83] AlexZander, "everything2," Everything2 Media, LLC, 18 March 2004. [Online]. Available: https://everything2.com/title/Pencil+lead. [Accessed 16 April 2018].

[84] A. Y. Khodakov, W. Chu and P. Fongarland, "Advances in the Development of Novel Cobalt Fischer−Tropsch Catalysts for Synthesis of Long-Chain Hydrocarbons and Clean Fuels," *Chemical Reviews,* vol. 107, no. 5, pp. 1692-1744, 2007.

[85] M. E. Dry, "Chemical concepts used for engineering prupose," *Studies in Surface Science and Catalysis ,* vol. 152, 2004.

[86] H. M. T. Galvis, A. C. Koeken, J. H. Bitter, T. Davidian, M. Ruitenbeek, A. I. Dugulan and K. P. de Jong, "Effect of precursor on the catalytic performance of supported iron catalysts for the Fischer–Tropsch synthesis of lower olefins," *Catalysis Today,* vol. 215, pp. 95-102, 2013.

[87] J. Bae, S.-M. Kim, S.-H. Kang, K. V. Chary and Y.-J. Lee, "Effect of support and cobalt precursors on the activity of Co/AlPO4 catalysts in Fishcer-Tropsch synthesis," *Journal of Molecular Catalysis A: Chemical,* vol. 311, pp. 7-16, 2009.

[88] O. J. Fabela II, "Effective Thermal Conductivity of Porous Media by Inverse Heat Transfer Analysis," The University of Texas at Arlington , Arlington, 2017.

[89] P. R. Ellis, D. James, P. T. Bishop, J. L. Casci, C. M. Lok and G. J. Kelly, "Synthesis of High Surface Area Cobalt-on-Alumina Catalsyts by Modification with Organic Compounds," *Catalysis,* vol. 128, no. 1, 2009.

[90] A. O. Odunsi, T. S. O'Donovan and D. A. Reay, "Dynamic Modeling of Fixed-Bed Fischer-Tropsch Reactors with Phase Change Material Diluents," *Chemical Engineering & Technology,* vol. 39, no. 11, pp. 2066-2076, 2016.

[91] A. A. Azzaz, A. A. Assadi, S. Jellali, A. Bouzaza, D. Wolbert, S. Rtimi and L. Bousselmi, "Discoloration of Simulated Textile Effluent in Contimuous Photoreactor using Immobilized Titanium Dioxide: Effect of Zinc and Sodium Chloride," *Journal of Photochemistry and Photobiology A: Chemistry ,* vol. 358, pp. 111-120, 2018.

[92] Y. Lu, P. Zhou, J. Han and F. Yu, "Fischer–Tropsch Synthesis of Liquid Hydrocarbons Over Mesoporous SBA-15 Supported Cobalt Catalyst," *Royal Society of Chemistry Advances,* vol. 5, pp. 59792-59803, 2015.

Biographical Information

Pawarat Bootpakdeetam received her Bachelor Degree in Mechanical Engineering from Kasetsart University, Bangkok, Thailand in 2008 and her Master Degree in Mechanical Engineering from the University of Texas at Arlington in 2013. She has been pursuing her PhD degree in Mechanical Engineering at the University of Texas at Arlington since 2013. Her research interests mainly include experimental study on sustainable energy development. Her research area involves coal pyrolysis, natural gas reforming, and Fischer-Tropsch synthesis.